ISSN 0376-5156
Geophytology 50(1&2): 11–36
May 2022

The ups and downs of palaeoaltimetric methods: The use of plant fossil and isotope proxies to determine past land surface height

Robert A. Spicer[1, 2, 3*] and Alex Farnsworth[2, 4]

[1]CAS Key Laboratory of Tropical Forest Ecology, Xishuangbanna Tropical Botanical Garden, Chinese Academy of Sciences, Mengla 666303, China.
[2]State Key Laboratory of Tibetan Plateau Earth System, Resources and Environment (TPESRE), Institute of Tibetan Plateau Research, Chinese Academy of Sciences, Beijing 100101, China.
[3] School of Environment, Earth and Ecosystem Sciences, The Open University, Milton Keynes MK7 6AA, UK. *E-mail: r.a.spicer@open.ac.uk
[4] School of Geographical Sciences, University of Bristol, University Road, Clifton, Bristol BS8 1SS, UK. E-mail: alex.farnsworth@bristol.ac.uk
*Corresponding author

Manuscript received: 23 March 2022
Accepted for publication: 30 March 2022

ABSTRACT

Spicer R.A. & Farnsworth A. 2022. The ups and downs of palaeoaltimetric methods: The use of plant fossil and isotope proxies to determine past land surface height. Geophytology 50(1&2): 11–36.

Tracking temporal changes in orography is of critical importance for modelling and understanding atmospheric, crustal and biodiversity dynamics over geological timescales, yet the different methodologies for doing this, while being complementary, are seldom compared and evaluated for a particular location at a known point in time. Here we explore the strengths and weaknesses of palaeoaltimetry as seen through the lenses of 1) altitude-related isotope fractionation (isotopic lapse rates), 2) changes in surface temperature with increasing elevation (terrestrial thermal lapse rates) and 3) conservation of energy principles. For our tests we use prior and new treatments of palaeoaltimetry proxies preserved in late Miocene to Pliocene deposits within the Zanda (Zhada) Basin, western Himalaya, now at a mean elevation of ~ 4200 m. In this setting, upslope lofting of pollen from the windward side of the Himalaya, lowers the perceived palaeoelevation of the basin to below 3.6 km, particularly when using a modern dry bulb thermal lapse rate. Erroneously low elevations are also given by such lapse rates applied to leaf fossil floras. The use of modelled Pliocene wet bulb terrestrial lapse rates increases the reconstructed basin height to plausible values similar to that of the present day, while energy conservation and isotope-based palaeoaltimetry give higher than present palaeoelevations. Any attempt to determine past surface heights requires a multiproxy approach because the different techniques reveal different aspects of past topographic relief.

Keywords: Isotopes, Plant fossils, Palaeoaltimetry, Himalaya, Climate modelling.

INTRODUCTION

Measuring the heights above mean sea level of ancient land surfaces is essential for informing our understanding of tectonic and atmospheric dynamics. Without quantifying such surface heights at known points in time we cannot compare, meaningfully, spatial patterns in temperature proxies, chart climate change, understand biodiversity origins or deduce deep Earth processes. Despite the critical nature of such measurements the methodologies employed are far from

© The Palaeobotanical Society, Lucknow, India

perfect, with uncertainties poorly quantified regarding both accuracy and precision. The aim of this paper is to evaluate the different palaeoaltimetric methods that have been used to document the topographic development of Earth's youngest, most extensive and highest orographic feature, the Himalaya-Tibetan Plateau complex, sometimes called 'Earth's Third Pole'. We do this by examining the performance of various palaeoaltimeters as applied to a young (late Miocene-Pliocene) depositional basin in the north-western Himalaya: the Zanda (Zhada) Basin.

Land surface elevation increases can be generated by the rise of rocks against the force of gravity, known as uplift, or by sediment infilling a basin (Molnar & England 1990). Unlike uplift, sediment infilling does not involve work against gravity, but it can, nevertheless, change a complex landform into a low relief plateau (so-called bathtub sedimentation, Tapponier et al. 2001). Uplift can be the result of lateral compression and thickening in the crust, or thermal processes, or both. Note that uplift is not the same as exhumation, which is the process of erosion, although in low temperature thermochronology exhumation is sometimes interpreted as surface rise.

Whatever the cause of the elevation of a land surface, air passing over that surface must have ascended from sea level and in so doing will have changed its properties, typically cooling as it rises and experiencing a rise in relative humidity as that cooling takes place. These atmospheric property changes can then propagate through the atmosphere generating rainfall, latent heat changes, and convection, possibly altering wind directions and ultimately affecting climate regionally and even globally, depending on the size and position of the topographic feature.

In today's world there is no greater obstacle to air flow than the Himalaya, and they provide a natural laboratory for testing a variety of methods for measuring surface height by means of geological proxies; proxies and methods that can then be applied more widely in palaeoaltimetry. Along the southern flank of the Himalaya the prevailing summer wind direction is from the south and south west, and as moist air from the Indian Ocean encounters the Himalayan obstacle some is deflected eastwards and some is forced upwards. Because pressure reduces with altitude any rising air parcel will expand and cool, and relative humidity will increase, often to an extent that generates rainfall. Moisture condensation gives off latent heat leading to convective rise of that air parcel, further cooling, and rain generation.

Commonly used palaeoaltimetric proxies exploit such atmospheric changes and in this paper we focus on two types of proxies: those based on changes in stable isotope ratios and those based on plant fossils. We examine the different methodologies used to transform proxy data into past surface heights and evaluate their strengths and weaknesses. As we shall see, where possible multiple methodologies should be used in conjunction because they offer different insights into past landscape evolution. Here the objective is to explore the relative performances of different approaches to the same palaeoaltimetric question in a setting appropriate to all the methods.

MEASURING THE HEIGHTS OF ANCIENT LAND SURFACES

To quantify surface elevation some measurement of a physical property of the environment that varies with height is required. Prior to GPS methods, modern surface heights were either derived by direct surveying or by exploiting the fact that air pressure declines with increasing elevation, a barometric measure. Although gas bubble size in lava has been looked at as a possible barometric palaeoaltimeter (e.g. Sahagian et al. 2002), this approach has not gained widespread adoption. More typical is the use of a geological proxy that records a systematic change in either temperature, combinations of temperature and humidity, or isotopic fractionation that takes place as evaporation and condensation cycles with increasing height. These are all forms of elevational lapse rates.

Stable Isotope Lapse Rates

Both hydrogen and oxygen naturally occur in the form of different stable isotopes. In the case of oxygen these are ^{16}O and ^{18}O. When water evaporates the lighter form (^{16}O) tends to pass from liquid to gas phase more easily than the heavier ^{18}O, so a parcel of air

above a water surface tends to be slighty enriched with this lighter istope compared to the source water body. Similarly when moisture condenses the heavier ^{18}O isotope tends to enrich any rain falling from a parcel of air leaving the air parcel isotopically lighter. This differential fractionation is the basis of isotope palaeolatimetry and exploits the fact that as a parcel of air rises against a mountain side progressive rain out of the heavier isotopes (they can be both oxygen and hydrogen) tends to follow a predictable 'Rayleigh fractionation' model (Figure 1) (Rowley et al. 2001, Poage & Chamberlain 2001, Rowley & Garzione 2007, Mulch 2016, Mulch & Chamberlain 2018).

Provided that the isotopic content of meteoric water (rain / snow) is preserved unaltered through time in a carrier substance (e.g. a mineral such as carbonate or an organic molecule) the elevation at which rainout occurred can be calculated provided that the isotopic composition of the air parcel at the start of its ascent, and an appropriate isotopic lapse rate following the Reyleigh fractionation model, are both known. Because the isotopic composition of sea water varies from place to place and over time, it is also essential to know where that source was and that the carrier material recording it is of the same age as the carrier at the altitude being investigated. This means that the track of the ancient air parcel needs to be known so that for any elevated sample the correct starting location, and thus original isotopic composition, is used for a baseline datum. In reality the height at which condensation actually takes place is not at the surface where carrier materials form but in convective clouds high in the atmosphere. Moreover, as a parcel of air traverses multiple mountain ranges the result of complex evaporation and condensation cycles, termed the 'continental effect', can be very difficult to quantify (Mulch 2016, Mulch & Chamberlain 2018). Despite these difficulties isotope palaeoaltimetry has become widely applied, even if this application often has to resort to largely unquantifiable 'educated guesses' regarding the underlying assumptions (Hoke 2018).

Thermal Lapse Rates

A commonly and long-used palaeoaltimetric proxy exploits the rate at which temperature declines with increasing height, and is known as a thermal lapse rate. When measured in a column of non-convecting 'free' air, this temperature decline is known as an environmental thermal lapse rate (Γ_e):

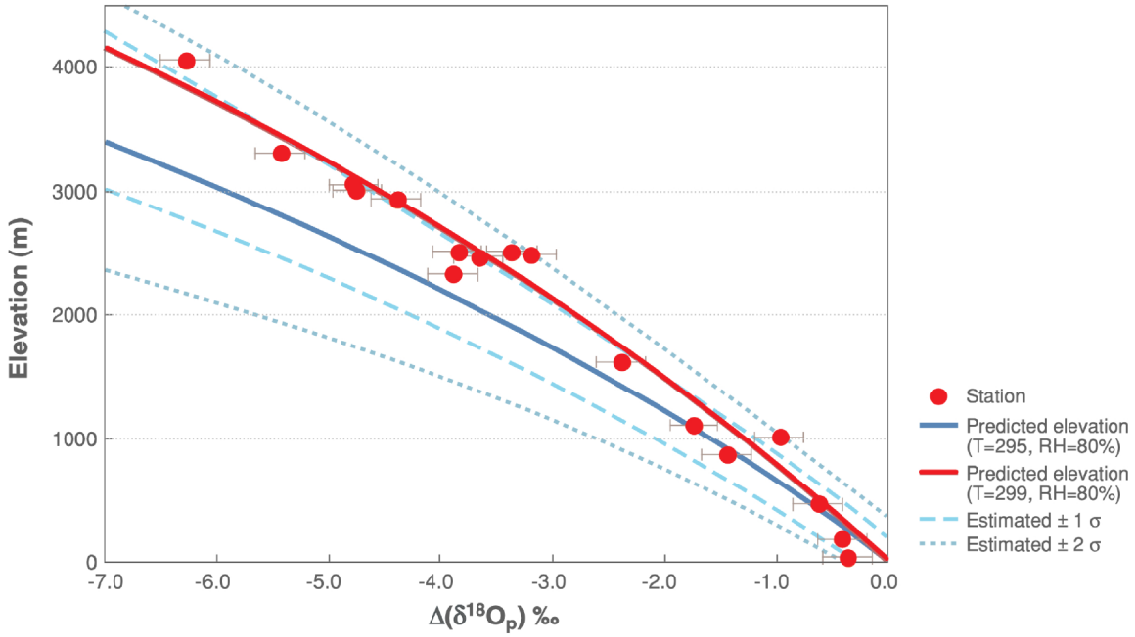

Figure 1. Exemplar Rayleigh condensation/fractionation model and station observations for oxygen isotopes showing altitude and temperature effects (Modified from Rowley & Garzione 2007).

$\Gamma_e = -dT/dZ$ *Eq. 1*

where *dT* isthe temperature difference measured over a height range (*dZ*). In today's world the global average Γ_e measured using a normal dry bulb thermometer is 6.5°C/km (Barry & Chorley 1987). However, this value is not globally uniform and varies from place to place and over time as the composition (particularly CO_2 and moisture content) of the atmosphere changes, so this value cannot be applied reliably to estimate past surface heights. Palaeoelevations based on this approach should be discarded.

Geological environmental proxies that record past environmental conditions do not form in a column of free air but near, on, or at shallow depths beneath, Earth's surface. A thermal lapse rate measured at such a surface, such as a mountainside, is termed a terrestrial thermal lapse rate (Γ_t) and differs from a free air thermal lapse rate in that surface temperatures are influenced by albedo, evapotranspiration, boundary layer turbulence and radiative processes. A lapse rate measured on a mountain side will vary with aspect and slope, and in an intermontane basin where temperature inversions often occur can even be negative (Meyer 1992, 2007, Wolfe 1992). Today the overall the global mean Γ_t is 5.5°C/km (Axelrod & Bailey 1976) reflecting a lower rate of cooling with increased height than the global mean Γ_e. Unfortunately, this mean figure is not very helpful because even in a spatially restricted region like the western USA it varies with altitude (0.3–3.6°C/km) and latitude (-4.9–4.5°C/km) (Wolfe 1992). Like Γ_e*s,* Γ_t temperatures are normally measured using a dry bulb thermometer.

Temperature Measurement Using Plant Fossils

Of course, we do not have direct thermometric measurements for the past and have, instead, to derive temperatures indirectly using proxies. Plant fossils are commonly used for this either by inferring temperatures based on the thermal tolerance of the nearest living relatives of the fossil taxa, or by looking at the correlations between plant physiognomy (architecture) and temperature (Spicer 2018). Plants are particularly valuable because they are exposed to, and interact directly with, the atmosphere near Earth's surface. As a consequence, they encode information about their immediate climate either in terms of the taxonomic composition of the community they are part of, or in their architecture. An example of the former (taxonomic) proxy is the Co-existence Approach (Mosbrugger & Utescher 1997, Utescher et al. 2014), while the latter encompasses tree ring analysis and leaf physiognomy, most notably the widely used Climate-Leaf Analysis Multivariate Program (CLAMP) (http://clamp.ibcas.ac.cn) (described and reviewed in Spicer et al. 2020b), and which does not require taxonomic identification. Unlike isotope proxies (carrier materials), plant fossils are not subject to diagenetic alteration, but are subject to taphonomic biases.

Temperature Measurement Using 'Clumped Isotopes'

In conventional stable isotope analysis an isotopic ratio (for example $^{18}O/^{16}O$) is measured with respect to that of a standard and the difference is expressed as permil (‰). In contrast to this approach, clumped isotopes reflect the relative proportions of different isotopes (isotopologues) in a mineral crystal lattice. The most common clumped isotope palaeothermometer measures the isotopologues of carbon and oxygen in CO_2 with a mass of 47 when it is released from carrier carbonates dissolved in phosphoric acid, i.e. when ^{13}C and ^{18}O are substituted for ^{12}C and ^{16}O. The amount of substitution or 'clumping' (Δ_{47}) is temperature dependant (Ghosh et al. 2006, Eiler 2007), with preferential clumping of the heavier isotopes (^{13}C and ^{18}O) taking place at lower temperatures. Note, however, that disequilibrium and 'vital' effects do occur (Affek et al. 2008, Zaarur et al. 2011).

Often the carbonates analysed are those precipitated as nodules at depth (> 40 cm) in fossil soils (palaeosols), and Δ_{47} values can be converted to air temperatures using an empirical dry bulb transfer function (Kelson et al. 2017). Using climate modelling and the Davies-Jones formula (Davies-Jones 2008) these dry bulb temperatures can then be converted to wet bulb temperatures (Xiong et al. 2022) which, as we shall see, can be particularly valuable in palaeoaltimetry. However, because carbonate precipitation only takes place when the soil is warm

and drying (Peters et al. 2013), the temperatures obtained are not annual means, but are biased towards those parts of the year when the carbonate is precipitated. These temperatures have often been assumed to reflect summer conditions, but this need not be the case (Peters et al. 2013, Xiong et al. 2022) as it also depends upon the local precipitation/ evaporation regime.

Dry Bulb and Wet Bulb Temperature Measurements

Earlier we referred to the fact that as a parcel of air rises its temperature tends to fall, and that this in turn leads to a rise in relative humidity. As it is extremely rare for the atmosphere to be completely dry, and humidity varies throughout the year linked to the annual cycle of temperature change, it follows that as a parcel of air traverses a topographically complex land surface any moisture it contained at the start of its journey will fluctuate as its temperature varies with height. Evaporation and condensation will also give rise to temperature variations as a function of latent heat exchange, and for this reason, dry bulb thermal lapse rates show poor skill in predicting surface height, at least in the context of numerical climate modelling (Farnsworth et al. 2021).

A far better predictor is a terrestrial lapse rate measured using a wet bulb thermometer because this temperature is also a function of moisture content. At saturation wet bulb and dry bulb thermometer readings are identical, but if a parcel of air is not moisture-saturated evaporation from a damp wick around a thermometer bulb will produce a temperature reading that is less than that of a dry bulb. The dry bulb - wet bulb temperature difference depends on how moisture-saturated the air is. Wet bulb terrestrial thermal lapse rates show considerable skill at reproducing prescribed topographies in a modelling context irrespective of the time of year when the proxy used to derive them is formed (Farnsworth et al. 2021). Fortunately, leaves more or less constantly loose water to the atmosphere through evapotranspiration and so function like a wet-bulb thermometer, which means leaf traits as scored in CLAMP code well for wet bulb temperatures (Figure 2a).

Conservation of Energy

Changes in temperature and moisture content within a parcel of air as it rises is also exploited in a palaeoaltimeter based on Newton's First Law of Thermodynamics: conservation of energy.

As a parcel of air rises its moist static energy (h), which is the sum of moist enthalpy (H) and potential energy, is conserved (Forest et al. 1995, 1999). Gains in height result in an increase in potential energy (gZ) so H must decrease. Mathematically h is expressed as:

$$h = c'_p T + Lv_q + gZ \qquad Eq.\ 2$$

where c'_p is the specific heat capacity at a constant pressure of moist air, T is temperature (in K), Lv is the latent heat of vaporization of water, q is specific humidity, g is acceleration due to gravity (a constant) and Z is elevation. H, then, represents a combination of temperature, moisture content and the latent heat that connects them.

More simply:

$$h = H + gZ \qquad Eq.\ 3$$

which can be rearranged so that any reduction in H from low elevation (H_{low}) to high (H_{high}) will give the height difference (ΔZ):

$$\Delta Z = (H_{low} - H_{high})/g \qquad Eq.\ 4$$

Because H is a function of both temperature and moisture not only is it a reliable palaeoaltimeter, but it is also something that plants respond to, and code for, in leaf form (Figure 2b).

The Growth of the Himalaya-Tibet Orogenic System

The palaeoaltimetric techniques outlined above have all been applied to try and quantify the growth of the Himalaya-Tibet edifice, sometimes called 'Earth's Third Pole' (Qiu 2008) because of the affect it has on regional atmospheric thermodynamics and ultimately global climate. This region includes not only the Himalaya and the high elevation low relief portion of Tibet, but also the topographically complex and highly biodiverse Hengduan Mountains on the eastern margin of the Tibetan Plateau.

Stable isotope fractionation palaeoaltimetry has been used to argue that central Tibet formed by a

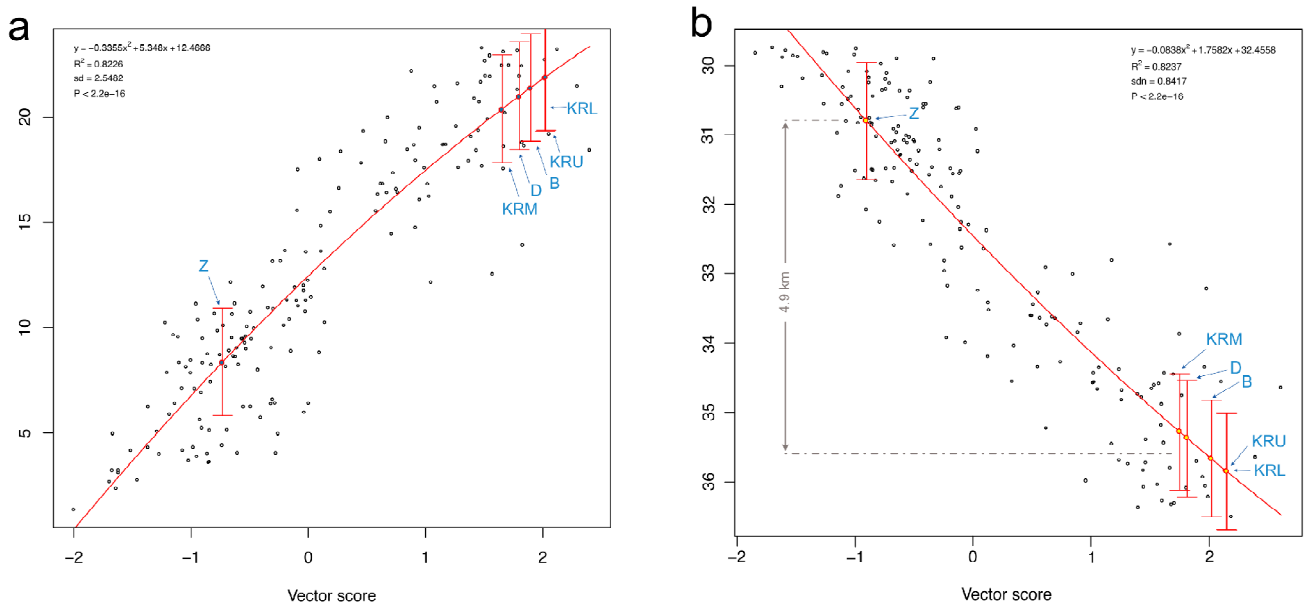

Figure 2. CLAMP PhysgAsia2/WorldClim2 regressions with calibration sites shown as open black circles, uncertainty bars indicate ±1 standard deviation; Z: Zanda Basin, KRL: Kameng River Lower (mid to late Miocene), KRM: Kameng River Middle (Pliocene), KRU: Kameng River Upper (late Pliocene-Pleistocene), B: Bhutan (late Miocene to Pliocene), D: Darjeeling (mid to late Miocene). **a**. Mean annual wet bulb temperature. **b.** Mean annual moist enthalpy showing the elevation difference between the Zanda Basin sample and the mean elevation of the Siwalik samples.

progressive rise from Southwest to Northeast (Rowley & Currie 2006, Mulch & Chamberlain 2006) in which southern Tibet and the Himalaya rose to exceed 4 km prior to 40 Ma, and that the Qaidam area was only uplifted as recently as the Pliocene. A rather different model envisages a similarly high Paleogene 'proto-Tibetan Plateau' expanding northwards and southwards in the Neogene (Wang C.-S. et al. 2008, 2014). However, these Paleogene high elevations in central Tibet are in stark contrast to the low (< 2 km) elevations

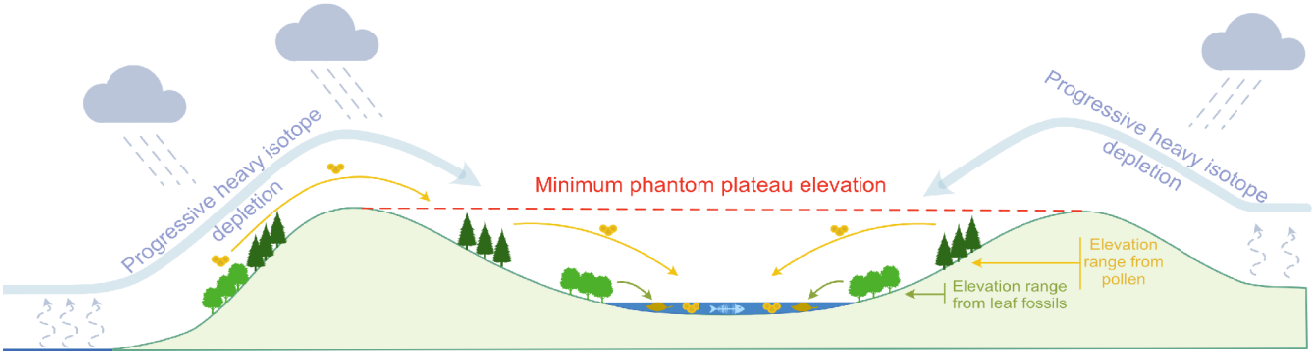

Figure 3. Cartoon showing the processes and outcomes of different palaeoaltimetric methods in a valley system under a monsoon (seasonally reversing air-flow) climate. Evaporation and condensation fractionate the isotopic composition of air parcels cresting mountain ridges, so isotope carrier materials within the valley all have a light isotope signature representing (at a minimum) the heights of mountain crests bounding the valley. Because all the within-valley carrier materials have a relatively light isotopic composition a 'phantom plateau' is produced. In contrast limited transport distances mean leaf fossils represent vegetation close to depositional sites (e.g. lake margins) in the valley lowlands, while pollen can be derived from a range of elevations, so giving an erroneous mean height for the valley floor. In addition, pollen can be lofted from low elevations external to the valley, potentially depressing the perceived valley floor height. Because the pollen sources cannot be accurately defined the elevation estimates they produce are unreliable (modified from Spicer et al. 2020a).

indicated by palaeontology (Deng & Ding 2015, Spicer 2020a and references therein),where recent analyses point to a wide (> 200 km) east-west trending central valley (Su et al. 2019, 2020, Xiong et al. 2022) as originally proposed by Ding et al. (2014) based on tectonic considerations. The disparity between stable isotope-predicted surface heights and those derived from fossils lies in what these different approaches actually measure.

In respect of isotopic lapse rates, because a parcel of air gets progressively depleted by rain-out of heavy isotopes as it rises against a mountain barrier, the air traversing that barrier into lowlands beyond carries with it the isotopically light composition that it inherited at the mountain range crest, or even higher in convective clouds. Formation of carrier compounds in that lowland will therefore indicate an elevation reflecting the height of the mountain crest (or higher), not that of the lowland depositional basin where they formed and became preserved. Where there is a central valley bounded by two mountain systems, for example in Paleogene Tibet where the Andean-type Gangdese mountains to the south and the Tanggula (Central Watershed) mountains to the north bounded the Tibetan Central Valley (Figure 3), coupled with a monsoon system of seasonally reversing airflows, only isotopically light air cresting either of the mountain barriers will enter the valley. Carrier materials formed in that central valley will therefore indicate a 'phantom plateau' with a pseudo-palaeoelevation reflecting the heights of the bounding mountain crests (Figure 3).

By contrast, fossils accumulating in the valley bottom sediments will, in the case of relatively easily degraded leaf material, be primarily derived from vegetation bordering the within-valley depositional sites (e.g. a lake) and thus reflect the temperature and moist enthalpy regime in the valley lowlands (Figure 3). Pollen, particularly that produced by wind-pollinated taxa that occupy higher elevations where the spring period for insect pollination is short, tend to have special morphologies (i.e. air sacs) that aid long distance dispersal. Moreover, wind-pollinated species tend to produce pollen in much larger quantities than insect-pollinated species. Such high elevation pollen entering the lake system by wind-blow or mountain stream-flow will indicate an anomalously high elevation for the basin floor, and certainly higher than that derived from using the more locally sourced leaf fossils (Figure 3). Note also that the use of typical pollen sampling devices or moss polsters (e.g. Cundill 1991, Hansen 1949) to calibrate pollen palaeoaltimeters will also misrepresent the elevation of ancient pollen sources because such sampling does not factor in downslope transport by water. Unsurprisingly then, conventional isotopic lapse rate and fossil palaeoaltimeters give different elevation estimates (Figure 3) (Deng & Ding 2015, Spicer et al. 2020a), particularly in valley systems.

In the case of a single mountain barrier, such as the pre-Himalaya Paleogene Gangdese mountain range along the southern border of what is now the Tibetan Plateau, the situation is less complex. Here, wet air drawn northwards by a heated Asian continental interior summer low pressure system will develop an isotopic signature reflecting both its original sea level composition and the fractionation height. For a basin on or near the crest of the mountain system it will be possible to measure that basin height, particularly if the carrier compounds (e.g. carbonates and leaf waxes) in such a montane basin are produced in the summer.

By contrast, in such a mountain system pollen can be lofted upwards on the windward slope (e.g. Zhang et al. 2017), and if this happens the montane basin pollen spectrum could well reflect a vegetation source growing below the basin height, so an anomalously low height will be returned for the basin. Any megafossils (e.g. leaves) preserved in such basins will still give a height estimate that differs from that derived from isotope fractionation, but in this case the difference reflects the relative mountain crest and basin lake elevations. This difference will, nevertheless, be useful to estimate past relief within the mountain chain. Thus, mid Miocene Gangdese height estimates given by isotopic fractionation and leaf form preserved in the Namling-Oiyug Basin are remarkably similar (Spicer et al. 2003, Khan et al. 2014, Currie et al. 2005, 2016, Polissar et al. 2009). Such a montane basin situation provides the ideal location for evaluating different palaeoaltimetric proxies, particularly in a younger basin where deep-

time changes in monsoon dynamics, topography and biology can be minimised. One such basin is the Zanda Basin in the north-western Himalaya.

THE MIOCENE-PLIOCENE ZANDA BASIN: A COMPARATIVE CASE STUDY IN PALAEOALTIMETRY

Geology, Age and Setting

The Zanda Basin (also referred to in the literature as the Zhada or Zhanda Basin) (Figure 4) (~ 31°N, 80°E, elevation 3990–4500 m) is located in the western Himalaya just south of the Yarlung-Tsangpo Suture and the ancient Gangdese Arc upland that lies along the southern margin of what is now the Tibetan Plateau. To the east the basin is bounded by the Gurla Mandhata gneiss dome and to the west the Leo Pargil dome. Within this 9,000 km^2 extensional basin ~ 900 m of late Neogene fluvial, lacustrine, aeolian and alluvial fan sediments have accumulated, derived in most part from the surrounding Gangdese and Himalaya. The sedimentary fill is tectonically undisturbed and overlies the deformed Tethyan sedimentary succession that elsewhere caps the High Himalaya. The entire basin sediment fill was originally referred to as the Zanda Formation (Zhang et al. 1981), but has since been subdivided into a lower Zanda Formation and an upper Xiangzi Formation (Qian 1999). Today the entire basin fill succession is eroded by the Langqen Zangpo (Sutlej) River, a tributary of the Indus, and this erosion affords sampling access to almost the complete succession (Figure 5).

Saylor et al. (2009) subdivided the succession into three parts reflecting different sedimentary environments. The lower 200 m exhibits trough cross-bedded sandstone and imbricated cobble conglomerates with 3-4 m thick bar foresets interpreted to represent deep large-scale rivers. Separating individual fluvial facies are laminated fine sands and silts containing abundant mammal, gastropod and plant fossils indicative of interfluve over-bank deposits. This

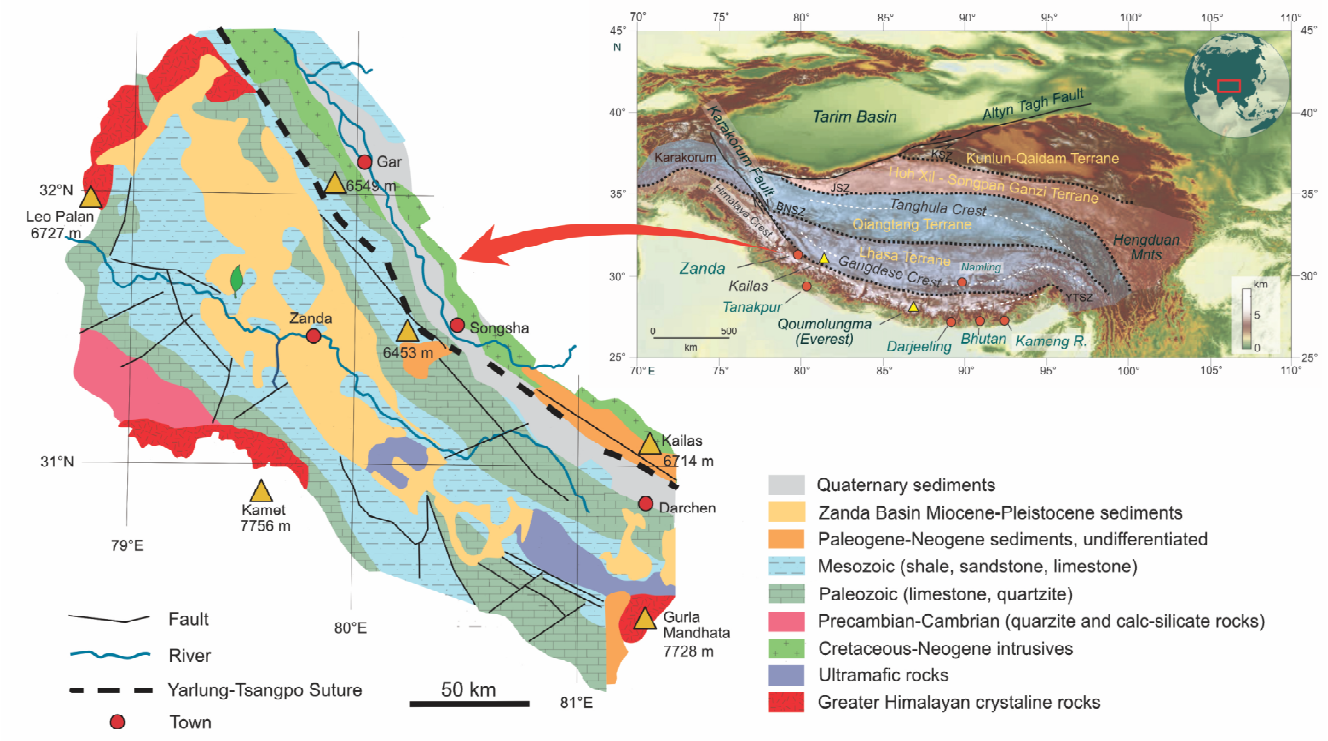

Figure 4. Map of the Tibetan region showing major terranes and key plant fossil localities mentioned in the text, and the geology of the Zanda Basin. The position of the Zanda Basin plant megafossil locality is indicated by the leaf symbol. Zanda Basin geology modified from Wu et al. (2014).

style of deposition suggests an open hydrological system.

The middle 250 m of the succession comprises a series of upward coarsening progradational lacustrine cycles each beginning with deep-water clays coarsening up to sands and conglomerates indicative of shallower depths. Some desiccation cracks and gypsum layers indicate episodes of drying. This pattern of deposition indicates a closed drainage system prone to periodic drying,

The upper 350 m also comprises upward coarsening sediments. Deepwater clays are replaced by deltaic or lake margin facies, including alluvial fan deposits. This suggests lake shallowing as the basin filled with sediments and a return to an open system in which rivers passed through the basin, as occurs today. This stratigraphy is summarised in Figure 5.

Palaeomagnetostratigraphy based on different sections has dated the succession as ranging from ~ 6 Ma to ~ 1.5 Ma (Zhang et al. 1981), ~7 – ~1Ma (Qian 1999), 9.5 to 2.6 Ma (Wang et al. 2008), and ~ 9.2 to 1 Ma (Saylor et al. 2009). Wang et al. (2013a) used a combination of magnetostratigraphy and mammalian fossils to date the onset of sedimentation as 6.4 Ma (Messinian, latest Miocene). The lowest 150m is regarded as latest Miocene, between 150 to 620 m the sediments are assigned to the Pliocene, and from 620 to 800 m to the Pleistocene. The overall age range is similar to results obtained by Deng et al. (2011, 2012), and therefore it seems that much of the succession spans the Pliocene (Figure 4).

The relatively young age of the basin fill sediments means that the proxy records they preserve were likely to have formed under conditions more similar to those of today that those of older basins such as Namling, particularly in terms of the tectonics and prevailing monsoon wind system. The location of the Zanda Basin,

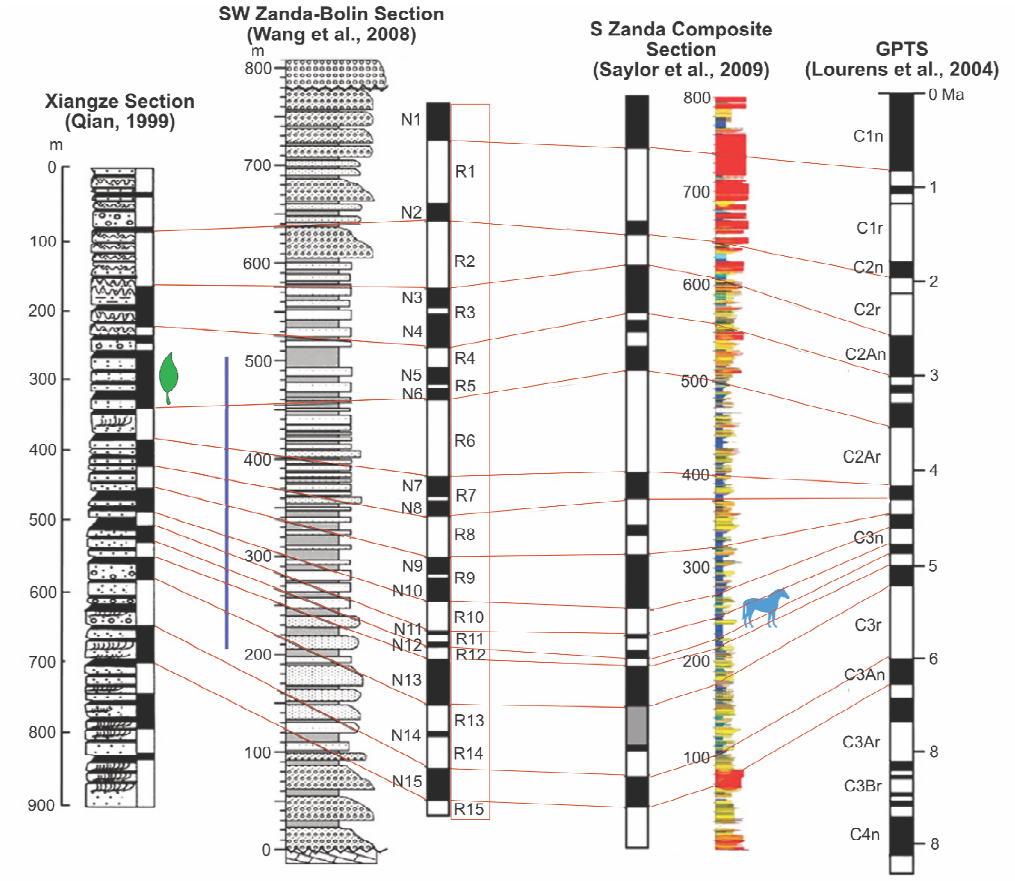

Figure 5. Composite stratigraphy of the Zanda Basin and temporal correlations, modified from Wu et al. (2014), showing the position of megaflora of Huang et al. (2020) (leaf symbol), palynoflora (blue line) and *Hipparion* fossil (Deng et al. (2012) (horse symbol). Modified from Wu et al. (2014).

just north of the Himalayan crest, means that today the waters draining into it likely only experience a single major elevation-related fractionation as northward moving wet air crests the Himalaya driven by the prevailing summer monsoon winds. Given ample evidence for the existence of a modern South Asian Monsoon in the Miocene (Bhatia et al. 2021a,b; Li et al. 2021, Farnsworth et al. 2019b) this situation is also likely to have existed in the late Miocene to Pliocene. It therefore offers a 'best case' scenario comparing isotope palaeoaltimetry with past height estimates derived from fossil proxies.

Proxies

The young age of the Zanda Basin and contained sediments reduces the likelihood of diagenetic alteration of the isotope carrier minerals and these are reported as being 'pristine' (Saylor et al. 2009). This provides an ideal setting for evaluating isotopic fractionation and should also preserve a reliable estimate of past carbonate formation temperatures using the 'clumped' isotope approach.

For palaeontological proxies (here primarily palaeobotanical) the catchment area sourcing potential megafossils (leaves, fruits and seeds) is more or less well-defined, both now and in the past, because of the young age of the basin. Moreover, the pollen record can easily be interpreted as many of the taxa are still extant, even at the species level. This is important because correct identification is critical in translating palynomorph records into temperatures, and pollen abundance/presence is subject to the usual problems of taxon-dependant differential production and dispersal. Extensive up- and down-slope transport of grains by wind and water within the catchment, including significant upslope transport on the windward side of a mountain barrier outside of the catchment (e.g. Zhang et al. 2017), in this case the Himalaya, is likely to have also occurred in the late Miocene-Pliocene. Knowing the general depositional setting is useful for understanding these potential taphonomic biases. This setting, therefore, provides a useful test of the typical palaeontological biases that affect a mountain basin.

MODERN CLIMATE AND VEGETATION OF THE ZANDA BASIN

Climate

Today the Zanda Basin experiences a cold temperate semi-arid climate, typified by cold dry winters and cool summers. There are no continuous records of modern climate measured within the Zanda Basin itself, so Saylor et al. (2009) used those recorded at Shiquanhe (Ali), some 117 km away to the NNW and at an elevation of 4378 m. Based on these data the modern (1969-1990) mean annual air temperature (MAT) for the Zanda Basin is projected to be 0°C, the average temperature between April and October is 7°C, while the warm month mean temperature (WMMT) is 14°C. Between 1961 and 1990 the WMMT was 13.7°C based on gridded data (Table 1). The modern average relative humidity there is 30 percent, reaching a maximum of 50 percent during the monsoon. These data were recorded over an interval of less than the 30 years required to be considered as a climate 'normal' so here we also use data with an underlying DEM to adjust for elevation (Table 1). Note while the gridded data and those used by Saylor et al. (2009) are in good agreement for where there is a recording station as at Shiquanhe, the scarcity of meteorological recording stations across the topographically complex Tibetan region means that these gridded data are less reliable in areas without a recording station, such as the Zanda Basin, than they would in more observation-rich parts of the world that exhibit less relief.

Vegetation

The modern vegetation of the Zanda Basin comprises sub-alpine desert grassland including a small proportion of shrubs with typical taxa being: *Stipa plareosa*, *Artemisia, Ephedra, Ceratoides latens* and *Salsola* (The comprehensive scientific expedition to the Qinghai–Xizang Plateau 1985). Wind-pollinated conifers such as *Pinus*, *Picea* and *Abies* are not present in the Basin, nor in the immediate surrounding area.

Table 1. Modern gridded climate data based on observations between 1961-1990 (New et al. 2002) for the Zanda Basin, Shiquanhe and selected Siwalik sites. MAT - mean annual air temperature, WMMT - warm month mean air temperature, CMMT - cold month mean air temperature, GSP - growing season precipitation, 3WET/3DRY - ratio of precipitation during the consecutive three wettest and three driest months, Enthalpy - mean annual moist enthalpy, Lat - latitude, Long - longitude, Elev - elevation.

Site Name	MAT (°C)	WMMT (°C)	CMMT (°C)	GSP (cm)	3WET/ 3DRY	Enthalpy (kJ/kg)	Lat (°N)	Long (°E)	Elev (m)
Zanda	1.95	12.42	-9.10	14.00	8.26	292.89	31.00	80.00	4250
Shiquanhe	-0.21	13.69	-12.64	3.8	10.83	291.36	32.497	80.104	4288
Kameng R.	24.30	28.89	16.48	182.59	23.42	353.31	26.92	92.61	200
Darjeeling	23.18	27.33	15.64	285.72	75.01	351.66	26.76	88.27	218
Bhutan	22.29	26.61	15.06	397.71	66.48	348.97	26.72	90.01	363
Tanakpur	24.33	31.54	14.54	172.35	20.48	346.20	28.89	80.17	200
Siwalik Mean	23.53	28.59	15.43	259.59	46.35	350.04			245

THE SIWALIK NEAR SEA-LEVEL DATUM

Elevation is normally measured from a sea level datum, so in palaeoaltimetry we require contemporaneous isotope / fossil proxies representing conditions at, or close to, sea level as well as at the height we are investigating. For the late Miocene to Pliocene Zanda Basin such near-sea level proxies can be found in the ~7000 m-thick succession of predominantly freshwater-deposited coarsely-bedded sandstone, siltstone, grit, clay and conglomeratic molassic deposits known as the Siwalik succession (Acharya 1994). These highly fossiliferous (Cautley 1835) Neogene sediments represent the erosional products of the rising Himalaya and were deposited in the Himalayan foreland basin today occupied by the Ganges River. Today the Gangetic Plain is barely more than 200 m above sea level and we assume the Siwalik depositional surface was at a similar, or lower, height in the late Miocene-Pliocene. Some Siwalik sediments contain fossil mangrove material (Mitra et al. 2000, More et al. 2016) showing they were deposited at sea level.

The Siwalik succession is generally divided into Lower, Middle and Upper Siwaliks (Medlicott 1864, Middlemiss 1890, Pilgrim 1913, Colbert 1934, 1942). Dating throughout the Siwaliks tends to be by magnetostratigraphy (e.g. Sangode et al. 2003, Kumaravel et al. 2005, Coutand et al. 2016). CLAMP analysis of the well-studied Siwalik megafloras (Pathak 1969, Antal & Awasthi 1993, Prasad 1994a, b, c, Prasad & Pandey 2008, Khan et al. 2011, 2014a, b; 2019) provides a detailed insight into the prevailing late Miocene to Pliocene sea level climate along the base of the Himalaya (Table 2).

The modern South Asia Monsoon (SAM) seems to have dominated the climate of India and southern Tibet since at least the beginning of the Neogene (Bhatia et al. 2021a, b; Li et al. 2021), although across central Asia the monsoonal climate differed from the modern SAM in ways yet to be fully understood (Su et al. 2019, 2020, Li et al. 2021). Across India an Inter Tropical Convergence Zone type monsoon, as experienced today in NE Australia and parts of Indonesia, persisted until the late Oligocene when a climate with the characteristics of the modern SAM began to emerge (Bhatia et al. 2021). By the latest Miocene a SAM similar to that of the present was well established, to which local vegetation along the southern Himalayan front had equilibrated, and this is reflected in fossil leaf form recovered from mid Miocene to Pleistocene Siwalik sediments (Khan et al. 2011, 2014 a, b, 2019) (Table 2).

MODERN CLIMATE AND VEGETATION OF THE SIWALIKS

Table 1 shows gridded modern climate data for selected Siwalik locations along the foot of the Himalayan front. Note that these are very similar to those obtained from the late Neogene proxies (Table 2), with the modern cold month mean being only slightly (by < 5°C) cooler.

Table 2. CLAMP-derived palaeoclimate data for Miocene and Pliocene Siwalik sites. Analyses are based on the PhysgAsia2/WorldClim2 calibration. At all sites the composition of the vegetation can be characterised as mostly evergreen broadleaved angiosperms. Abbreviations as for Table 1.

Age and References	MAT (dry) (°C)	MAT (wet) (°C)	WMMT (°C)	CMMT (°C)	GSP (cm)	3WET/ 3DRY	Enthalpy (kJ/kg)
1. Zanda Basin (~ 3.5 Ma) (Huang et al. 2020)	16.89	8.38	28.83	3.65	111.06	9.3	307.8
2. Mid to late Miocene (15–10 Ma) Kameng River Flora, eastern Siwaliks, N. India (Khan et al. 2014a; Srivastava et al. 2018)	25.17	21.9	28.01	20.70	196.41	11.3	358.5
3. Mid to late Miocene (15–10 Ma) Darjeeling Flora, eastern Siwaliks, N. India (Antal &Awasthi 1993, Antal & Prasad 1996a, b, 1997, 1998, Awasthi 1992, Khan et al. 2014a)	24.2	21.01	28.2	18.6	237.2	4.7	353.5
4. Pliocene (5.3–3 Ma) Kameng River, middle Siwaliks, eastern Himalaya (Khan et al. 2014a)	23.3	20.39	27.3	18.2	200	7.7	352.7
5. Late Miocene-Pliocene Bhutan (Khan et al. 2019)	24.2	21.41	27.3	20	188.4	9.6	356.5
6. Late Pliocene to Pleistocene (3 Ma–0.01 Ma) Kameng River, upper Siwaliks, eastern Himalaya (Khan et al. 2014a)	25.0	21.9	28.0	20.3	208.2	10	358
Siwalik Mean	24.4	21.3	27.8	19.6	206.5	13.6	355.8
Uncertainty	2.36	2.5	2.91	3.54	64.32	8.7	0.84

Today lowland Siwalik vegetation comprises tropical moist semi-evergreen forest elements, including *Pongamia pinnata*, *Duabanga grandiflora*, *Callistemon lanceolatus*, *Terminalia catappa*, *Terminalia chebula*, *Terminalia miocarpa*, *Litsea* spp., *Bauhinia purpurea*, *Albizia* spp., *Michelia champaca*, *Gynocardia odorata*, *Syzygium* spp., *Dipterocarpus* spp., *Aglaia argentea*, *Gmelina arborea*, *Ficus* spp., *Calophyllum polyanthum*, *Cinnamom umbejolghota*, *Actinodaphne angustifolia*, *Actinodaphne obovata*, *Alstonia scholaris*, *Bombax malabaricum*, *Bombax ceiba*, *Macaranga denticulata*, *Knema* spp., *Bischofia javanica*, *Canarium strictum*, *Dalbergia sisso*, *Anthocephalus cadamba*, *Elaeocarpus aristatus*, *Elaeocarpus rugosus*, *Phoebe goalparensis*, *Meliosma simplicifolia*, *Turpinia nepalensis*, *Lagerstoemia parviflora*, *Quercus lamellosa*, and *Croton chlorocalyx* (Hazra et al. 1996).

STABLE ISOTOPE LATE NEOGENE HEIGHT MEASUREMENTS OF THE ZANDA BASIN

In respect of isotopic studies, we adopt previous elevation estimates using conventional stable oxygen and carbon isotopes from carbonates (gastropods shells and palaeosol nodules) (Saylor et al. 2009), and carbonate clumped isotope thermometry of gastropods, tufas and palaeosol nodules (Huntingdon et al. 2015). We refer readers to these works for details of the isotope methodologies, particularly because the assumptions involved are numerous and complex, but we summarise the approaches here for convenience.

Saylor et al. (2009) collected modern water samples from 20 locations throughout the Zanda Basin and in some cases sampling was continued over several years. No rain fell in the basin during the field campaigns so water sampling was from the Sutlej River, a nearby tributary of the Tsangpo River, and from small springs within the basin. Samples were also taken from wetland ponds. These modern $\delta^{18}O_{sw}$ (surface water) values ranged from -17.9 to -11.9 permil (VSMOW). Modern gastropod shells were taken from the shorelines of nearby wetland ponds. δ^{13}Ccc (carbonate) values of gastropods ranged from -13.8 to -7.5 permil and covaried with δ^{18}Occ (carbonate), which ranged from -20.3 to +0.2 permil (VPDB).

To obtain late Miocene and Pliocene isotopic signatures at the sea level start of the moisture pathway to the Zanda Basin Saylor et al. (2009) assumed an Indian summer monsoon system deriving moisture from the south, and that sea level temperatures over both land and ocean were similar to those of present, which they justified on the grounds that MATs derived from Miocene carbonate nodules in western Nepal (26.5°C) (Quade et al. 1995) and NLR estimates from Siwalik plant fossil assemblages (specifically using Awasthi & Prasad 1989, Sarkar 1989, but see also Table 2) are close to today's observed temperatures (Table 1) in the Himalayan foreland basin. These temperatures are important because they impact evaporation and the $\delta^{18}O$ versus elevation lapse rate.

If isotopic measurements from geological materials (carbonate from nodules shells, bone or organic matter from plant remains) are to reflect the isotopic ratios of the ancient meteoric water, those materials (isotopic carriers) must remain unaltered over time. Saylor et al. (2009) tested for diagenesis and concluded that the Zanda fossil gastropod shells were pristine. However, while fossil gastropods from fluvial settings seemed in general to reflect meteoric water, those from lacustrine environments were evaporatively enriched, consistent with the preserved mudcracks and gypsum.

Estimates for temperatures at which carbonate formation occurs are typically based on the MAT, but in the cooler climates encountered at higher altitudes this may not be appropriate (Huntingdon et al. 2015). Saylor et al. (2009) assumed that the Zanda gastropods had grown mostly in the summer months, and in a series of complex arguments concluded that using modern climate parameters for the Zanda Basin was valid for interpreting the isotopic compositions of the fossil material. Detailed temperature measurement for shallow freshwater conditions for rivers and ponds in the Zanda region today are lacking, so they had to be inferred from air temperatures recorded at Shiquanhe, and using such data they set the aragonite formation temperature to be +7°C, with a seasonal variation of ±7°C that equated to a 1.5 per mil uncertainty for all the samples. If the actual carbonate formation was warmer, this would lower the palaeoelevation estimate. For low elevations at the start of the moisture pathway Saylor et al. (2009) derived palaeosurface water $\delta^{18}O_{psw}$ values from palaeosols preserved in the Siwaliks of Pakistan and Nepal (Quade et al. 1995, Dettman et al. 2001). As within the Zanda Basin, low elevation moisture is derived in part from multiple glacier sources and groundwater, as well as local precipitation. The same ± 1.5 per mil uncertainty due to seasonal changes in the temperature of carbonate formation was applied as for the Zanda Basin. Initially Saylor et al. (2009) also had to modify the previously published theoretical Rayleigh fractionation (Rowley et al. 2001, Rowley & Garzione 2007) and empirical (Garzione et al. 2000) models because the modern water samples plotted above the $\Delta^{18}O_{sw}$ versus elevation curves (effectively the isotopic lapse rates). Adjustments were made by accounting for a change in isotopic composition of $\delta^{18}O_{sw}$ in the Siwaliks due to enhanced glacial melting during the past 100 years (Thompson et al. 2000).

The palaeoelevation obtained by Saylor et al. (2009) is given in Table 3 and shown graphically as the light pink band in Figure 6.

Clumped Isotopes

Clumped isotopes offer way of resolving the uncertainties surrounding the late Miocene-Pliocene carbonate formation temperatures in the Zanda Basin recognised by Saylor et al. (2009). Using palaeosol carbonate, aragonitic gastropods and tufa from the Zanda Basin Huntingdon et al. (2015) re-examined its elevation at ~4 Ma because of concerns over uncertainties surrounding the temperature of gastropod carbonate (aragonite) formation within the ancient Zanda Basin.

The clumped isotope palaeoelevation obtained by Huntington et al. (2015) is given in Table 3 and Figure 6.

FOSSIL AND THERMAL LAPSE RATE ESTIMATES OF THE LATE NEOGENE ELEVATION OF THE ZANDA BASIN

Spores and Pollen

Following on from an earlier study (Li & Liang 1983) Wu et al. (2014) reported on the Pliocene pollen

Table 3. Comparative results for the different palaeoaltimetric techniques applied to determine the late Miocene-Pliocene surface height of the Zanda Basin.

Type of Study	Assumed age (Ma)	Palaeoelevation	References
Modern Observation	0	3.5–4.5 km (basin floor) > 6 km (peaks)	
Stable isotope ($\delta^{18}O$, carbon)	~ 9	5–6 km (catchment) 1–1.5 km higher than present	Saylor et al. (2009)
Clumped isotopes	8.5–3.7	4.9–5.4 ± 0.5 km (catchment) 1.5 ± 0.5 km higher than present	Huntington et al. (2015)
Clumped Isotope wet bulb MAT with a model-derived mean annual wet bulb terrestrial lapse rate (3.56°C/km)	8.5–3.7	4.6– 5.8 (mean 5.25) km	Huntington et al. (2015) modified here.
CA (Megafossil) dry bulb lapse rate	3–3.5	3.5–4.2 km (basin floor)	Huang et al. (2020)
CA (Pollen/Spores) implied modern dry bulb lapse rate	2.3–5	<3.6 km	Wu et al. (2014)
CLAMP (moist enthalpy)	3–3.5	5.2km (basin floor)	This paper
CLAMP (MAT dry bulb, global mean free air lapse rate dry bulb)	3–3.5	1.6 km	This paper
CLAMP (JJA terrestrial lapse rate dry bulb)	3–3.5	2.5 km	This paper
CLAMP (MAT dry bulb, local terrestrial lapse rate wet bulb)	3–3.5	2.4 km	This paper
CLAMP (MAT wet bulb, CLAMP-derived local wet bulb lapse rate)	3–3.5	3.6 km	This paper
CLAMP (MAT wet bulb, local terrestrial model-derived wet bulb lapse rate)	3–3.5	3.9 km	This paper

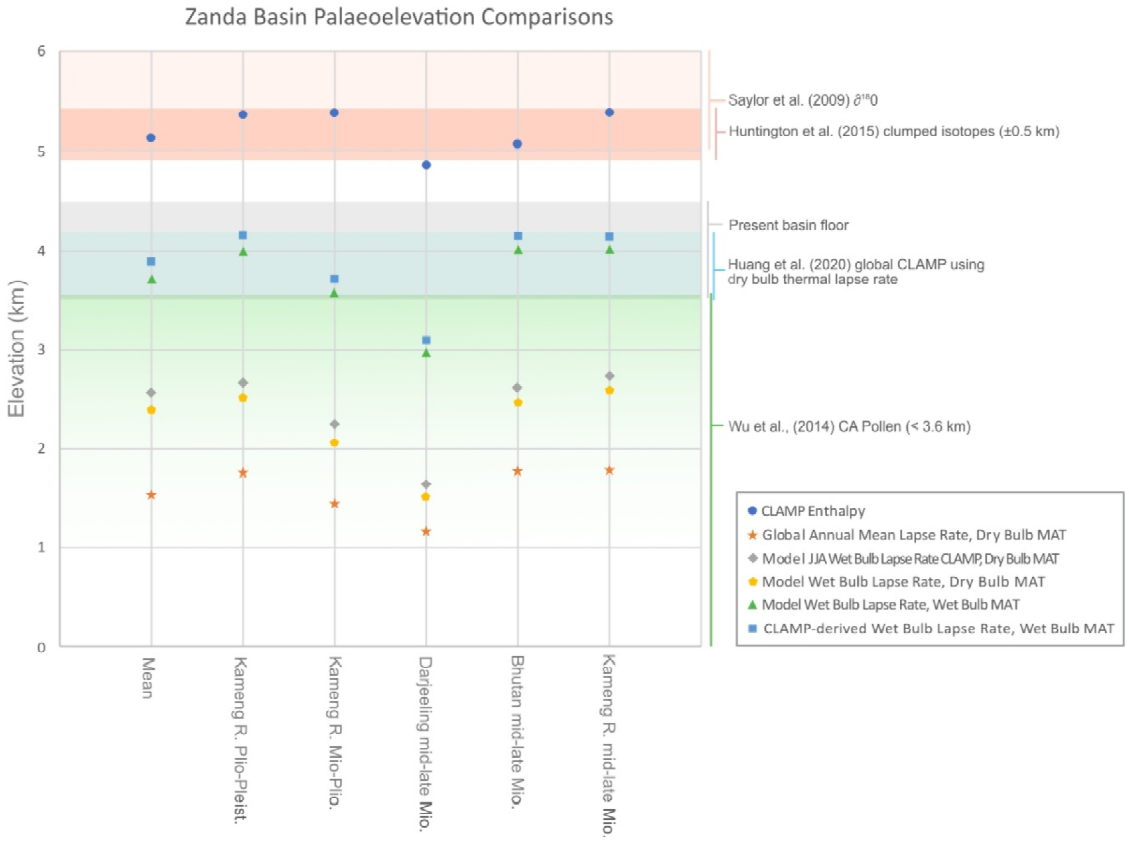

Figure 6. Summary of results of previous palaeoaltimetric estimates in the literature compared with the present analyses using moist enthalpy and thermal lapse rate approaches. Global mean and local terrestrial model-derived dry and wet-bulb thermal lapse rates are included. Siwalik fossil sites are only those where there is confidence that they were near sea level when they were deposited. A baseline elevation of 250 m is assumed for these sites for consistency.

and spore flora from the Zanda Basin. The assemblage, dated at 4.7 - 3.6 Ma and comprising 71 taxa, was dominated by conifer tree species: *Pinus* (2–51.2%, av. 27.2%), *Picea* (up to 54.3%, av. 24.2%), *Abies* (3.2–50.76%, av. 21%), *Podocarpus* (av. 5.2%), and *Cedrus*, *Tsuga*, as well as grains representing *Taxodiaceae*/*Cupressaceae*/*Taxaceae* which occur only occasionally. Angiosperms make up only a small proportion of the overall assemblage (averaging just 2.6%) with trees such as *Tilia*, *Betula*, *Melia*, *Juglans*, *Quercus*, *Ulmus*, *Carya*, *Pterocarya*, and *Castanea* occurring with subordinate shrub and herbaceous taxa including Compositae (*Anthemis*-, *Aster*-, *Saussurea*-, and *Taraxacum*-types - average 1.1%), *Artemisia*, *Gramineae*, *Rosa*, *Ericaceae*, *Ephedra*, *Chenopodiaceae*, and *Cyperaceae* and lycophyte and fern spores representing *Lycopodiaceae* (average 3%), *Pteridaceae* (average 4%), and *Polypodiaceae* (average 4.4%).

For height estimates based on palynology we refer to the work of Wu et al. (2014), who relied upon the modern elevation ranges of 18 mostly conifer taxa that grow within the Tibetan region as whole. They then adjusted these by ~4°C, a figure derived from warmer Pliocene ocean temperatures (but where and at what depth we are not told) of 2-3°C adjusted for temperature differences generally being greater at higher altitudes than at sea level (Bradley et al. 2006). The pollen-based height estimates of Wu et al. (2014) are given in Table 3 and Figure 6.

Megafossils

Huang et al. (2020) collected a megafossil (predominantly leaves) flora from the location shown in Figure 4, which was deposited at ~ 3.5 Ma (Figure 3). The assemblage comprises 87 specimens and was recovered from a single 1.5 m thick horizon within grey-whitish silty mudstone sediments exposed in a river bank 2 km to the east of Laga village (31.726042°N, 79°561853°E, 3990 a.m.s.l.). Stratigraphically this is in the upper middle part of the Zanda Formation, and Huang et al. (2020) regard the age to be 3-3.5 Ma, using the geomagnetic polarity time scale of Lourens et al. (2004).

Most Zanda Basin fossil leaves are small, falling between the nanophyll (12%) and mesophyll 1 (38%) size classes using the CLAMP categorizations (http://clamp.ibcas.ac.cn). This suggests the source vegetation was either dominated by shrubs adapted to semi-arid conditions, as is the case today in the Zanda Basin, or that there was significant taphonomic filtering that favoured only small xeromorphic leaves being preserved. This can happen in open lake settings (Spicer 1981, Ferguson 1985).

This Xiangzi flora represents 21 species belonging to 12 genera in 10 families. In contrast to the pollen flora of Li & Liang (1983) and Wu et al. (2014), no conifer megafossil remains have been found. The most abundant taxa in terms of numbers of specimens were *Cotoneaster*, *Spiraea* and *Caragana*, followed by *Hippophae*, *Rhododendron* and *Potentilla fruticosa*. Less common woody taxa included *Salix*, *Lonicera*, *Ceratostigma*, and *Berberis* as well as herbaceous groups such as *Polygonum* and *Kobresia*. Overall the flora appears drought-adapted and typical of deciduous shrubs with wide ecological tolerances allowing them to grow on hillsides, plains and along rivers. However, the flora also includes some taxa (*Lonicera*, *Hippophae, Kobresia and Polygonum*) that are better suited to locations where moisture is more abundant, for example around lake margins. While the drought-adapted nature of the Pliocene flora appears similar to that found in the Zanda Basin today, the taxonomic composition is slightly different in that *Cotoneaster*, *Spiraea*, *Potentilla fruticosa* are rare in the Zanda Basin today.

The Xiangzi Flora formed the basis for a CLAMP analysis conducted by Huang et al. (2020) and here we use the trait scores published by them, but unlike Huang et al. (2020) who used a global CLAMP calibration we analysed these traits using the more locally appropriate PhysgAsia2 physiognomic training set, combined with Worldclim2 gridded climate data.

Huang et al. (2020) also used the Co-existence Approach (CA) (Mosbrugger & Utescher 1997, Utescher et al. 2014) based on distribution data acquired from the Global Biodiversity Information System (GBIF, http://www.gbif.org/) and WorldClim (http://www.worldclim.org), climate data at a spatial

resolution of 30' × 30' (Fick & Hijmans 2017). Climatic envelopes and altitude ranges for each taxon were calculated using the Bioclimatic Envelope Model within the R software Dismo package. Finally, co-existence analysis was performed using R software.

Because modern altitudinal ranges were used in the Huang et al. (2020) elevation estimate it intrinsically involved a modern lapse rate and required correcting for Pliocene conditions. To reduce the large uncertainties associated with mean annual lapse rates Huang et al. (2020) used cold month mean temperatures Thus:

$$Z_{fossil} = Z_{NLRs} + (MTCM_{Pliocene}/\Gamma_{tPliocene})$$

where $MTCM_{Pliocene}$ is the difference in the coldest month mean dry bulb temperature (MTCM) between the Pliocene and present based on a HadCM3 model simulation (-0.1095°C) and where Z_{NLRs} is the modern elevation occupied by the nearest living relatives. Their result using this approach is given in Table 3 and in Figure 6.

MOIST ENTHALPY ELEVATION ESTIMATES FOR THE ZANDA BASIN

Huang et al. (2020) derived moist enthalpy from the physiognomy of the Xiangzi fossil flora using conventional CLAMP scoring. Overall the fossil flora represents a small- leaved shrub community in which nanophyll and leptophylls predominate. Most leaves had rounded apices and a short or absent petiole. Nanophylls accounted for 12% of the size range, Leptophyll I 24%, Leptophyll II 26%, and Microphyll I 38%. The largest leaves (belonging to *Hippophae*) were only 3–4 cm long.

To obtain climate data Huang et al. (2020) used the CLAMP Global 378 calibration, but did not specify which climate data set they used, and in general the climate variables were similar to those obtained by CA. However, they did not attempt to determine the palaeoelevation using moist enthalpy. Here we use Xiangzi leaf physiognomic traits as scored by Huang et al. (2020) to derive moist enthalpy, but we use CLAMP calibrated using PhysgAsia2 with WorldClim2 (Fick & Hijmans 2017) climate data. This gives a more precise result than the more generic Global 378 training data as has been used widely across Asia (e.g. Khan et al. 2014, Su et al. 2019, 2020, Bhatia et al. 2021a, b).

To derive sea level moist enthalpy we analysed a range of Siwalik fossil floras, also using the PhysgAsia2 and Worldclim2 CLAMP calibration (Table 2). The elevation results are given in Table 3 and graphically in Figure 6.

CLIMATE MODELLING

With the exception of Huang et al. (2020), all the previous studies have assumed that the late Miocene to Pleistocene climate of the Zanda Basin was similar to that of the present day, using proxy data to justify this assumption. However, this means that modern day lapse rates were assumed, as were moisture pathways. To explore if this is a reasonable assumption we employ a climate model.

A geologic Stage-level climate simulation for the Piacenzian (Pliocene; ~3 Ma.) was carried out using the HadCM3BL-M2.1aE model, a version of the HadCM3 coupled atmosphere-ocean general circulation model (AOGCM) (Valdes et al. 2017). The HadCM3BL climate model has a horizontal resolution of 2.5° latitude x 3.75° longitude in the atmosphere and ocean, with a vertical resolution of 19 levels in the atmospheric component and 20 levels in the oceanic component (Valdes et al. 2017). It is similar to the HadCM3L climate model, which has been utilised in numerous palaeoclimate (e.g. Farnsworth et al. 2019a, Saupe et al. 2019) and palaeoaltimetry studies (e.g. Su et al. 2019, Farnsworth et al. 2021), but differs in its reduced ocean resolution. This divergence from the HadCM3L is necessary due to the considerable spin-up times required for climate simulations to equilibrate to different climates and boundary conditions (land-sea distribution, topography, bathymetry, solar luminosity, land-ice distribution and pCO_2) in deep time (Farnsworth et al. 2019). This is crucial and often neglected, but is a requirement to ensure that ocean temperatures and, in turn, ocean circulation is fully representative of all applied forcings which can take many thousands of years to have an impact, such as on deep bottom water temperatures. The Piacenzian stage-level palaeoclimate simulation was run for 10,422 years, reaching both surface and deep-water equilibrium.

This model also provided local dry bulb and wet bulb lapse rates, which in conjunction with wet and dry bulb temperatures derived from CLAMP analysis of the leaf fossils, can also be used to derive palaeoelevation estimates.

RESULTS

CLAMP low elevation climate results derived from the late Miocene-Pleistocene Siwalik fossil floras are given in Table 2, while the palaeoelevation results for the different methodologies are shown in summary form in Table 3 and Figure 6. For Table 2, Siwalik sites were selected for those most likely to have been within 250m of sea level when they were deposited based on their current low elevation and/or evidence of marine influence. We assume none have decreased in height since they were formed. Only Siwalik assemblages of similar age to the Zanda Basin sediments were considered for the palaeoaltimetry tests.

Isotopes

The isotope models used by Saylor et al. (2009) predicted a minimum decrease in elevation of the Zanda Basin of between 0.6 (+0.2/-0.3) km and 0.8 (+0.3/-0.4) km since the Pliocene, and that in the Pliocene the mountains surrounding the basin were at least as high as today (>6,000 m). With all the uncertainties and assumptions taken into account, Saylor et al. (2009) concluded the elevation decrease within the Zanda Basin could have been as much as 1.5 km.

In their re-examination of carbonate formation temperatures using clumped isotopes Huntingdon et al. (2015) measured the temperature ($T\Delta_{47}$) at which the Miocene-Pliocene gastropod shells formed as being 8 ± 2 °C to 16 ± 2°C, with an average of 11 ± 3°C, which is somewhat warmer than the 7°C assumed by Saylor et al. (2009) and closer to the modern mean summer maximum air temperatures of ~ 12°C (Table 1) and the 17°C reconstructed for the Pliocene warm month mean air temperature using CLAMP and the leaf flora (Table 2). Other carbonates found at these altitudes, such as tufas, also show that they formed closer to summertime temperatures than MATs. $T\Delta_{47}$ values for modern and Holocene gastropods collected near to the Zanda Basin at elevations between 4810 and 4830 m were translated into modern Zanda Basin temperatures using an unspecified thermal lapse rate of 6.1°C/km. The fossil gastropods recovered from the Zanda Basin gave $T\Delta_{47}$ values 11 ± 3°C and so cooler than the summer temperature of 14°C inferred for the present by Saylor et al. (2009) using the Shiquanhe data. Using more rigorous interpolation of gridded observations the summer (warm month mean) temperature today is 12.4°C for an elevation of 4,500 m (Table 1). By again applying the 6.1°C/km lapse rate, and assuming no regional climate change, Huntington et al. (2015) derived a Miocene-Pliocene minimum basin elevation of 4.9 to 5.3 km, some 1.5 to 1.8 km ± 0.5 km (2s) higher than present (Table 3, Figure 6).

The dry bulb calibrated $T\Delta_{47}$ values of 11 ± 3°C obtained by Huntington et al. (2015) can be converted to wet bulb temperatures and an elevation estimate obtained using a model-derived Pliocene wet bulb terrestrial lapse rate (3.56°C/km). Using the 30% mean annual relative humidity given by Saylor et al. (2009) for the Zanda Basin the Davies-Jones formula gives a mean annual wet bulb temperature of 2.6°C, which when subtracted from the mean CLAMP mean annual wet bulb temperature in the Siwaliks resolves to an elevational difference of 5.25 km. When added to the Siwalik baseline elevation this suggests a Zanda Basin absolute elevation of 5.5 km. This is within the elevational bounds given by both Saylor at al. (2009) and Huntington et al. (2015) and close to that derived from moist enthalpy (Table 3, Figure 6).

Plants

Surface height estimates returned by thermal lapse rates and moist enthalpy derived from plant fossils, both pollen and leaves, range from 1.6 km and 5.2 km. The modern elevation of the Zanda Basin is in the range of 3990–4500 m depending on the location, and we would assume a Pliocene elevation to be similar this. This modern elevation provides a target against which to evaluate the different phytopalaeoaltimetric techniques.

The pollen-based approach of Wu et al. (2014), calibrated against modern vegetation zonation, not in the Himalaya but in eastern Tibet, yields an elevation no higher 3.6 km. Although Wu et al. (2014) did not specify it, a dry bulb terrestrial mean annual thermal

lapse rate specific to that region is implied. Within this broad elevational zone (green shading in Figure 6) we find other dry bulb mean annual temperature-based elevation estimates based on CLAMP analyses of leaf megafossils, irrespective of whether they are transformed to elevations using wet or dry bulb lapses rates (global or local). Note that the absolute elevation estimates vary depending on which Siwalik location was used for the sea level datum. In the illustrative samples used here these differences range over ~ 1 km.

The leaf fossil-derived estimates of Huang et al. (2020), based on a dry bulb lapse rate but with secular climate change adjustments, are somewhat higher at between 3.5 km and 4.2 km (blue shading on Figure 6), which is close to, but slightly lower than the modern elevational range within the basin (grey shading). Also falling within this range are height estimates based on CLAMP-derived wet bulb mean annual temperatures and model-derived local wet bulb terrestrial thermal lapse rates. The only exception is the estimate using the Darjeeling sea level datum, which gives low predictions for all methodologies and may reflect taphonomic or sampling biases in the Darjeeling sample.

CLAMP-derived moist enthalpy values yield elevations almost identical to those of Huntington et al. (2015) (dark pink shading in Figure 6) using temperatures derived from clumped isotopes, an elevational range nested within those of Saylor et al. (2009) (light pink shading) using isotopic fractionation. Note however, that although these authors used dry bulb lapse rate estimates they reduced estimation uncertainties by measuring late Neogene surface heights relative to those of the Zanda Basin today, and not a sea level datum, thus minimising the effects of differences in lapse rates because of the shorter vertical distances involved.

DISCUSSION

There have been several attempts to measure the palaeoelevation of the Zanda Basin using a variety of methods. Combined with new approaches and climate modelling, these legacy studies provide an opportunity to compare and evaluate palaeoaltimetric methodologies in an ideal geological setting afforded by the relatively young age of the basin. These studies also provide proxy data that can be used to apply new techniques. To evaluate these studies we assume that the Pliocene elevation was similar to that of the present day with an average within-basin surface height of ~ 4200m.

Isotope Palaeoaltimetry

The principle underlying this approach is that oxygen ($\delta^{18}O$) or deuterium (δD) compositions of meteoric (rain/snow) water ($\delta^{18}O_{mw}$ or δD_{mw}) vary as a function of elevation (Garzione et al. 2000, Rowley & Garzione 2007, Poage & Chamberlain 2001). Using stable isotopes to estimate past surface height demands numerous assumptions (Mulch 2016, Mulch & Chamberlain 2018), some of which have been described as 'educated guesses' (Hoke 2018). A primary requirement for stable isotope palaeoaltimetry is that the isotopic composition of the 'carrier' material (carbonate minerals formed in soils, lakes etc., or biologically mediated as in shell formation, plant waxes etc.) reflects accurately the original meteoric water isotopes and has not been altered, typically by burial (heating leading to re-crystalization and/or exchange of isotopes with the surrounding rocks) or exchange with more recent meteoric waters since deposition. One advantage of the Zanda Basin is the lack of deep burial (< 1 km) and Saylor et al. (2009) demonstrated that pristine aragonite shell material is preserved, which should record the primary isotopic composition of a variety of aquatic environments. In that study carbonate in some gastropod shells occupying fluvial conditions were assumed to preserve the isotopic composition of meteoric water captured by the drainages spanning a range of elevations feeding the Zanda palaeolake, while those living in the lake also reflected fractionation due to evaporation. At times evaporation was extreme, as evidenced by the evaporites and mudcracks, and in general lacustrine shells yielded higher $\delta^{18}O$ values than those from the river sediments reflecting loss of the lighter isotopes through this evaporation.

Another basic component of stable isotope analysis is that a localised isotopic lapse rate needs to be established, and this is usually done by comparison with isotopic variations in modern water in or near the site under investigation. Because the Zanda Basin is arid

today very little rain/snow falls directly into the basin, so for calibration purposes Saylor et al. (2009) measured $\delta^{18}O_{mw}$ in modern river and spring water feeding into the basin. As such, this included both modern precipitation falling high in the catchments, as well as glacial meltwater and groundwater that will have recorded fractionation that took place not only at high elevations but also over an extended time interval. The assumption is that because the basin seems to have been arid since the Miocene the same supplies would have operated in the Pliocene.

Normally, stable isotopic lapse rates observed today have to be adjusted for any changes in climate that may have taken place since the isotope carriers were formed. In the case of the Zanda Basin Saylor et al. (2009) argued that no significant change has taken place. They justified this assumption based on a lack of evidence for change in $\delta^{18}O$ compositions in the low elevation Siwaliks since the Miocene, and the persistence of a South Asian Monsoon circulation since that time. This assumption also meant that the same source and pathway existed in the late Miocene to Pliocene as in the present, allowing them to reconstruct the low elevation palaeosurface water isotopic composition ($\delta^{18}O_{psw}$) at the start of the air parcel trajectory. Potentially this also allows the use of modern $\delta^{18}O$ versus elevation relationships as observed (Garzione et al. 2000) and modelled (Rowley et al. 2007, Rowley & Garzione 2007).

One assumption crucial to isotope palaeoaltimetry concerns the temperature at which the carbonate forms and this depends on the type of carbonate. For shallow water micrites and tufas there is a distinct warm season bias and this bias increases with elevation (Huntington et al. 2010). To some extent this is also true for shallow water gastropod shells with only around 10% of shell formation in Tibetan species of *Radix* taking place in the winter months (Taft et al. 2013). However, the actual carbonate formation temperature is very much dependant on the preferred habitat of individual species, which may not be well constrained for extinct taxa. Saylor et al. (2009) used the modern Mean Annual Air Temperature (MAT) as measured at Shiquanhe (32.5°N, 80.083°E, 4280 m) between 1969 and 1990. This value of 0°C was used to estimate a mean warm season (April-October) temperature for aragonite precipitation of 7°C, but adjustments for evaporation also needed to be made and the different oxygen contributions from pre-monsoon and monsoon moisture. Overall there was a limited range of relative humidity, isotopic enrichment and temperature conditions compatible with both Miocene and modern climate. Despite, or perhaps because of, all these adjustments and assumptions (and others not discussed here) Saylor et al. (2009) found that the modern water samples from the Zanda area exceeded those predicted by both the Rayleigh fractionation model and empirical data from Nepal, meaning that the models became unreliable predictors of absolute elevation, and in particular that any palaeoelevation derived from such a relationship was only likely to be a minimum. Using fractionation models with two different low elevation starting temperatures did, however, provide a consistent relative estimate that the Zanda Basin in the Miocene-Pliocene was up to 1.5 km higher than present.

Huntington et al. (2015) revisited the Zanda Basin palaeoelevation estimates of Saylor et al. (2009) and used clumped isotopes to explore and document the gastropod carbonate formation temperatures in a more rigorous way. First, they analysed $T\Delta_{47}$ in modern and Holocene settings in Tibetan lakes 0.5-1 km higher than the present Zanda Basin and applied a (presumably dry-bulb) thermal lapse rate to estimate carbonate formation temperatures for the elevation of the modern Zanda Basin site. This lapse rate correction yielded Zanda Basin surface water temperatures 1–6°C warmer than those in the reference modern/Holocene lakes. The late Miocene-Pliocene fossil material, however, yielded much colder $T\Delta_{47}$ temperatures (by 11 ± 3°C) than the modern ones estimated from the thermal lapse rate. This suggests that either the late Miocene-Pliocene climate was cooler, or that the Zanda Basin was higher, or some combination of these causes. Huntingdon et al. (2015) considered that secular climate being cooler in the Miocene-Pliocene was unlikely given that other data suggest a general cooling has taken place over the past 9 million years, citing Zachos et al. (2001) and the lack of evidence for significant change in the Siwaliks

(Thomas et al. 2002, Quade et al. 2013). However, because the global temperature change of Zachos et al. (2001) is a deep ocean record, and may not be translatable to land surfaces (Pound & Salzmann 2017), and secular climate change is expressed more strongly at high elevations (Bradley et al. 2006), the minimal resolvable change at low elevation does not mean that change at height was unlikely. The regional climate regime of the late Miocene-Pliocene needs to be explored in more detail using climate modelling, but a comparison of Tables 1 and 2 shows that the modern climate is cooler than that of the Miocene-Pliocene in the Siwaliks, but this cooling is expressed most obviously in the winter months.

To translate the cooler temperatures into a height difference relative to present Huntingdon et al. (2015) applied a modern thermal lapse rate (by implication Γ_t but this is not specified) of 6.1°C /km. This gave a surface height reduction of 1.5 to 1.8 km ± 0.5 km (2σ) (the difference depending on the data analysed) and inferred a minimum average basin floor palaeoelevation of 4.9 to 5.5 km between 8.5 and 4.2 Ma.

Palynology and Thermal Lapse Rates

What is clear from the pollen and spore assemblage composition is that it is dominated by wind-pollinated taxa (Li & Liang 1983, Wu et al. 2014). That is to say, many of the pollen taxa possess features such as air sacs that enhance the likelihood that they will remain suspected in air for some time. Wind pollination serves all the conifers and most of the arboreal angiosperms present in the reported Zanda Basin assemblage. Insect pollination tends to be exploited by the shrubs and herbs while the lycophytes and ferns also rely on wind to disperse their spores, which tend to be small and hence have lower settling velocities than the larger pollen transferred between plants by insects. It is also clear that the pollen /spore spectrum is taxonomically distinct from that comprising the leaf flora. While the pollen assemblages are dominated by conifers (averaging 77% of the total abundance in all samples) conifers are absent from the leaf flora.

The palaeoelevation estimate of Wu et al. (2014) (Figure 6) was significantly lower than lose obtained by the other techniques (<3600m) and was derived from the modern altitude ranges of 18 conifers today found in the Tibetan region, mostly south-eastern Tibet, and not in the Himalaya where conifers form a significant proportion of the tree-line forests. Given the air parcel trajectories in the western Himalaya it is likely that these Himalayan trees were the source of the conifer component found in the Pliocene Zanda Basin, and as such do not reflect the basin elevation as assumed by Wu et al. (2014). Most of the wind-pollinated arboreal pollen taxa today live at elevations between 2000 and 4000m in eastern Tibet (as cited by Wu et al.,2014) so this will bias their elevation downwards irrespective of the appropriateness of their implied lapse rate assumptions.

The Leaf Flora

The Zanda Basin leaf megafossil flora consists of 21 species belonging to 12 genera distributed across 10 families (Huang et al. 2020). This assemblage was subjected to both the Co-existence Approach (CA) and a Climate-Leaf Analysis Multivariate Program (CLAMP) investigation to reconstruct palaeoclimate.

Using the climatic tolerances of the nearest living relatives (NLRs) of fossil taxa to determine palaeoclimate is the oldest form of palaeobotanical climate proxy, and the first record of its use was in 1086 by the Chinese scholar Shen-kuo (Needham 1986). NLR techniques can be applied to any identifiable plant organ (leaves, pollen/spores, fruits, seeds and wood). A fundamental assumption of this proxy is that little or no evolution has taken place, so it works best for assemblages that are relatively young (Neogene) (Utescher et al. 2014). A very young age (<5 Ma), as in the case of the Zanda Basin, also means that many fossil taxa will be morphologically similar to their presumed living relatives and so can be accurately identified. CA could, therefore, potentially yield reliable climatic results for the Pliocene Zanda leaf assemblage. The accuracy and precision of the results depends in part on the modern observations used to determine the climatic tolerances of the NLRs. In their analysis Huang et al. (2020) used the Global Biodiversity Information System (GBIF, http://www.gbif.org/) with a gridded Global Climate Model (WorldClim, http://

www.worldclim.org, resolution 30' × 30') (Fick & Hijmans, 2017) processed using the Bioclimatic Envelope model of the Dismo Package in R software. This is a more rigorous approach than Wu et al. (2014) used to estimate palaeoelevation from the pollen.

To derive the palaeoelevation of the vegetation sourcing the Zanda leaf assemblage Huang et al. (2020) using the altitudinal range of the modern NLRs modified by a correction for Pliocene conditions based on plant tolerances for the cold month mean temperature together with a Pliocene dry bulb thermal lapse rate derived from a numerical climate model (HadCM3BL). It is not clear from their paper if this was a global average free air lapse rate, or a local terrestrial lapse rate. Their reconstructed palaeoelevation was 3536–4176 m and as such is higher than, and barely overlaps with, the estimate derived from pollen.

Although fossil leaf floras will, on average, have undergone less transport than pollen from source to deposition, the elevation estimated from leaves depends very much on the metrics recovered from them and the technique used to transform these metrics into surface heights. Using global mean dry bulb temperatures from leaves, as usually retrieved in a standard CLAMP analysis, translates into low elevations irrespective of whether wet bulb or dry bulb lapse rates are used (Figure 6). This is the case even when wet bulb lapse rates are those of the summer season when most leaves will be functional and the prevailing winds from the south produce, in this setting, the ideal meteorological conditions to estimate elevation. Such conditions are those assumed in the isotope palaeoaltimetry, so it might be expected that there would be more agreement between the techniques than is actually the case.

Higher elevation estimates, closer to those of the Zanda Basin today, are obtained when CLAMP returns wet bulb mean annual temperatures using the Zanda leaf fossils combined with either a model-derived mean annual wet bulb lapse rate for the Pliocene (here specifically Piacenzian boundary conditions) or a wet bulb mean annual lapse rate derived from the difference between the mean Siwalik mean annual wet bulb temperatures and the mean annual wet bulb temperature of the Zanda Basin leaf fossil assemblage divided by the modern height difference. This dual comparison shows that the model is likely behaving realistically in a form comparable with the CLAMP proxy.

The highest leaf-derived elevation estimates are those obtained using moist enthalpy and these values match closely those derived from isotopic techniques measured relative to the modern elevation of the Zanda Basin. Moist enthalpy and isotopic palaeoaltimetry suggest higher elevations for the basin than present, but here it is worth considering again where exactly isotopic fractionation takes place and the source of the waters being analysed. The isotopic composition of air and water entering the basin will reflect the crest height of the upwind Himalayan barrier (Figure 3), and water deposited in the headwaters of the drainages feeding the within-basin lake/river system. In the case of the Zanda Basin this also includes water stored in glaciers. It is perhaps inevitable then that the elevation estimates exceed that of the basin floor.

This crest height elevation bias does not obviously apply to the moist enthalpy approach. To explore a potential bias in the moist enthalpy method we can simply subtract the moist enthalpy of the Zanda Basin today as derived from gridded climate data, from that of the modern Siwalik near sea level datum derived from the same dataset and then divide by the gravitational constant (g).When we do this using the Siwalik mean we find the predicted elevation of the Zanda Basin is 5.8 km (Table 1), some 1.5 km higher than the observed. When corrected for the fact that the Siwalik sites themselves are not at sea level the over-estimation increases further. This over estimation of height may be due to the fact that today the western Siwaliks are drier than those further east, so to test this we can use a Siwalik location closer to the longitude of the Zanda Basin. Such a site is Tanakpur, and when we use this datum the estimate is still 5.4 km or ~1.4 km higher than the basin when corrected for the Tanakpur elevation (200m) (Table 1). So, it seems that moist enthalpy estimates in this setting exceed the actual basin elevation by at least 1 km. Further work is required to explore this phenomenon.

CONCLUSIONS

No palaeoaltimeter is perfect and all have inherent strengths and weaknesses. Perhaps the most unreliable are those based on fossil pollen simply because of the potentially protracted transport distances involved, both up and down slope, and the recalcitrant nature of pollen. Combined with inappropriate and often unspecified lapse rates, either inferred from modern elevation-related vegetation zones or directly applied dry bulb global or local thermal lapse rates, this approach is likely to give wildly unreliable outcomes. They will deliver a numerical elevation estimate, but the uncertainties will be unquantifiable and the number will be meaningless.

If we accept that the Pliocene elevation of the Zanda Basin is likely to have been similar to that of the present then wet bulb thermal lapse rates, combined with wet bulb temperatures derived from leaf physiognomy, seems to give one of the most reliable palaeoaltimetric estimates. Such an approach does, however, rely on accurate numerical modelling to derive a wet bulb local terrestrial thermal lapse rate. Similar results can be obtained using taxon-based (CA) temperatures, but the methodology used by Huang et al. (2020) was complex and lacked the physical underpinnings of the wet-bulb lapse rate approach (Farnsworth et al. 2021). Recalibration of taxon-based approaches to yield wet bulb temperatures may offer a way forward.

It is quite clear that isotopic fractionation palaeoaltimetry will be biased towards crest heights encountered by an air parcel on its pathway to where proxies are likely to be preserved. Even in a best-case scenario this assumes that that the pathway, and thus starting point isotope ratio, is accurately known, and that the proxies faithfully retain the original meteoric isotopic signature. Nevertheless, inferring crest heights can be useful for comparison with the basin floor heights likely to be reflected in megafossil assemblages. Where isotopic approaches cannot be used reliably is in situations where reversing monsoonal airflows pass over a valley system because this will falsely indicate a plateau with a 'phantom' height similar to the heights of the bounding mountain systems.

Moist enthalpy/conservation of energy palaeoaltimetry is theoretically most robust and straightforward, particularly because moist enthalpy is coded strongly in leaf form. However, as we have seen in the Zanda Basin context there is a tendency to over-estimate elevations and it is not immediately obvious why. Further work is necessary to understand this, similar to that done recently on wet-bulb terrestrial lapse rates (Farnsworth et al. (2021), but if it turns out height exaggeration is systematic, then it can be corrected for.

Based on the uncertainties surrounding the various palaeoaltimetric methods it is not yet possible to say precisely what the late Miocene to Pliocene elevation of the Zanda Basin was, or whether the basin height has reduced in the last 3 million years or so.

ACKNOWLEDGEMENTS

We are grateful for the invitation to contribute to this special issue and for numerous colleagues in India for their work collecting, scoring and publishing trait data for Siwalik leaf assemblages. This work was support by an XTBG International Fellowship for Visiting Scientists to R.A.S., and the NSFC–NERC (Natural Environment Research Council of the United Kingdom) joint research program [nos. 41661134049 and NE/P013805/1]. This is a NECLIME contribution.

REFERENCES

Acharya S.K. 1994. The Cenozoic foreland basin and tectonics of the Eastern Sub-Himalaya: problem and prospects. Himalayan Geology 15: 3–21.

Affek H., Bar-Matthews M., Ayalon A., Matthews A & Eiler J. 2008. Glacial/interglacial temperature variations in Soreq cave speleothems as recorded by clumped isotope thermometry. Geochimica et Cosmochimica Acta 72: 5351–5360.

Antal J.S. & Awasthi N. 1993. Fossil flora from the Himalayan foot hills of Darjeeling foot-hills of Darjeeling District, West Bengal and its palaeoecological and phytogeographical significance. Palaeobotanist 42: 14–60.

Antal J.S. & Prasad M. 1996a. Dipterocarpaceous fossil leaves from Gish River section in Himalayan foothills near Oodlabari, Darjeeling district, West Bengal. Palaeobotanist 43: 73–77.

Antal J.S. & Prasad M. 1996b. Some more leaf-impressions from the Himalayan foothills of Darjeeling district, West Bengal, India. Palaeobotanist 43: 1–9.

Antal J.S. & Prasad M. 1997. Angiospermous fossil leaves from the Siwalik sediments (Middle-Miocene) of Darjeeling district, West Bengal. Palaeobotanist 46: 95–104.

Antal J.S. & Prasad M. 1998. Morphotaxonomic study of some more fossil leaves from the lower Siwalik sediments of West Bengal, India. Palaeobotanist 47: 86–98.

Awasthi N. 1992. Changing patterns of vegetation through Siwalik succession. Palaeobotanist 40: 312–327.

Awasthi N. & Prasad, M. 1989. Siwalik plant fossils from Surai Khola area, western Nepal. Palaeobotanist 38: 298–318.

Axelrod D.I. & Bailey H.P. 1976. Tertiary vegetation, climate, and altitude of the Rio Grande depression, New Mexico–Colorado. Paleobiology 2: 235–254.

Barry R.G. & Chorley R.J. 1987. Atmosphere, Weather, and Climate. 8th ed. Methuen, 50 pp, 8th ed. Routledge, New York, p. 421.

Bhatia H., Srivastava G., Spicer R.A., Farnsworth A., Spicer T.E.V., Mehrotra R.C., Paudayal K. & Valdes P.J. 2021. Leaf physiognomy records the Miocene intensification of the South Asia Monsoon. Global and Planetary Change 196: 103365. https://doi.org/10.1016/j.gloplacha.2020.103365.

Bhatia H., Khan M.A., Srivastava G., Hazra T., Spicer R.A., Hazra M., Mehrotra R.C., Spicer T.E.V., Bera S. & Roy K. 2021. Late Cretaceous–Paleogene Indian monsoon climate vis-à-vis movement of the Indian plate, and the birth of the South Asian Monsoon. Gondwana Research 93: 89–100.

Bradley R.S., Vuille M., Diaz H.F. & Vergara W. 2006. Threats to water supplies in the tropical Andes. Science 312: 1755–1756.

Cautley P.T. 1835. Letter noticing the discovery of further fossils in vast quantity in the Siwalik Range. Journal of the Asiatic Society of Bengal 4: 585–587.

Colbert E.H. 1934. A new rhinoceros from the Siwalik formations in north-western Himalayas. Sedimentary Geology 8: 77–82.

Colbert E.H. 1942. The geological succession of Proboscidae. Proboscidae 2: 142–152.

Coutand I., Barrier L., Govi G., Grujic D., Hoorn C., Dupont-Nivet G. & Najman Y. 2016. Late Miocene-Pleistocene evolution of India-Eurasia convergence partitioning between the Bhutan Himalaya and the Shillong Plateau: new evidences from foreland basin deposits along the Dungsam Chu section, eastern Bhutan. Tectonics 35: 2963–2994.

Cundill P.R. 1991. Comparisons of moss polster and pollen trap data: a pilot study. Grana 30: 310–308.

Currie B.S., Polissar P.J., Rowley D.B., Ingalls M., Li S., Olack G. & Freeman K.H. 2016. Multiproxy paleoaltimetry of the late Oligocene-Pliocene Oiyug Basin, Southern Tibet. American Journal of Science 316: 401–436.

Currie B.S., Rowley D.B. & Tabor N.J 2005. Middle Miocene paleoaltimetry of southern Tibet: implications for the role of mantle thickening and delamination in the Himalayan orogen. Geology 33: 181–184.

Davies-Jones R. 2008. An efficient and accurate method for computing the wet-bulb temperature along pseudoadiabats. Monthly Weather Review 136: 2764–2785.

Deng T. & Ding L. 2015. Paleoaltimetry reconstructions of the Tibetan Plateau: progress and contradictions. National Science Review 2: 417–437. https://doi.org/10.1093/nsr/nwv062.

Deng T., Li Q., Tseng Z.J., Takeuchi G.T., Wang Y., Xie G., Wang S., Hou S. & Wang X. 2012. Locomotive implication of a Pliocene three-toed horse skeleton from Tibet and its paleoaltimetry significance. Proceedings of the National Academy of Sciences 109: 7374–7378.

Deng T., Wang X., Fortelius M., Li Q., Wang Y., Tseng Z.J., Takeuchi G.T., Saylor J.E., Saila L.K. & Xie G. 2011. Out of Tibet: Pliocene woolly rhino suggests high-plateau origin of Ice Age mega herbivores. Science 333: 1285–1288.

Dettman D.L., Kohn M.J., Quade J., Ryerson F.J., Ojha T.P. & Hamidullah S. 2001. Seasonal stable isotope evidence for a strong Asian monsoon throughout the past 10.7 m.y.: Geology 29: 31–34. doi:10.1130/0091-7613.

Ding L., Xu Q., Yue Y.H., Wang H.Q., Cai F.I. & Li S.Q. 2014. The Andean-type Gangdese Mountains: Paleoelevation record from the Paleocene–Eocene Linzhou Basin. Earth and Planetary Science Letters 392: 250–264.

Eiler J.M. 2007. "Clumped-isotope" geochemistry–The study of naturally-occurring, multiply-substituted isotopologues: Earth and Planetary Science Letters 262: 309–327. doi: 10.1016/j.epsl.2007.08.020.

Farnsworth A., Lunt D.J., O'Brien C.L., Foster G.L., Inglis G.N., Markwick P., Pancost R.D. &.Robinson S.A. 2019a. Geophysical Research Letters 46(16): 9880–9889.

Farnsworth A., Lunt D.J., Robinson S.A., Valdes P.J., Roberts W.H.G., Clift P.D., Markwick P., Su T., Wrobel N., Bragg F., Kelland S.-J. & Pancost R.D. 2019b. Past East Asian monsoon evolution controlled by paleogeography, not CO_2. Science Advances 5: eaax1697.

Farnsworth A., Valdes P.J., Spicer R.A., Ding L., Witkowski C., Lauretano V., Li S.-F., Li S.-H. & Zhou Z.-K. 2021. Palaeoclimate model-derived thermal lapse rates: towards increasing precision in palaeoaltimetry studies. Earth and Planetary Science Letters 564: 116903 https://doi.org/10.1016/j.epsl.2021.116903

Ferguson D.K. 1985. The Origin of Leaf assemblages–new light on an old problem. Review of Palaeobotany and Palynology 46: 117–188.

Fick S.E. & Hijmans R.J. 2017. WorldClim2: new 1-km spatial resolution climate surfaces for global land surfaces. International Journal of Climatology 27: 4302–4315.

Forest C.E., Molnar P. & Emanuel K.E. 1995.Palaeoaltimetry from energy conservation principles. Nature 343: 249–253.

Forest C.E., Wolfe J.A. & Emanuel K.A. 1999. Paleoaltimetry incorporating atmospheric physics and botanical estimates of paleoclimate. Geological Society of America Bulletin 111: 497–511.

Garzione C., Quade J., DeCelles P. & English N. 2000. Predicting paleoelevation of Tibet and the Himalaya from delta $\delta^{18}O$ vs. altitude gradients in meteoric water across the Nepal Himalaya: Earth and Planetary Science Letters 183: 215–229. doi:10.1016/S0012 -821X(00)00252-1.

Ghosh P., Adkins J., Affek H., Balta B., Guo W., Schauble E., Schrag D. & Eiler J. 2006. ^{13}C-^{18}O bonds in carbonate minerals: A new kind of paleothermometer. Geochimica et Cosmochimica Acta 70: 1439–1456.

Hansen H.P. 1949. Pollen content of Moss Polsters in relation to forest composition. The American Midland Naturalist 42: 473–479.

Hazra P.K., Verma D.M. & Giri G.S. (Eds.) 1996. Materials for the flora of Arunachal Pradesh. Botanical Survey of India 1, pp. 13–22.

Hoke G.D. 2018. Geochronology transforms our view of how Tibet's southeast margin evolved. Geology 46: 95–96.

Huang J., Su T., Li S.-F., Wu F.-X., Deng T. & Zhou Z.-K. 2020. Pliocene flora and paleoenvironment of Zanda Basin, Tibet, China. Science China Earth Sciences, 63: 212–223.

Huntington K.W., Saylor J., Quade J. & Hudson A.M. 2015. High late Miocene–Pliocene elevation of the Zhada Basin, southwestern

Tibetan Plateau, from carbonate clumped isotope thermometry. G.S.A. Bulletin 127: 181–199.

Huntington K.W., Wernicke B.P. & Eiler J.M. 2010. Influence of climate change and uplift on Colorado Plateau paleotemperatures from carbonate clumped isotope thermometry. Tectonics 29: TC3005, doi:10.1029/2009TC002449.

Kelson J.R., Huntington K.W., Schauer A.J., Saenger C. & Lechler A.R. 2017. Toward a universal carbonate clumped isotope calibration: Diverse synthesis and preparatory methods suggest a single temperature relationship. Geochimica et Cosmochimica Acta 197: 104–131.

Khan M.A., Bera M., Spicer R.A., Spicer T.E.V. & Bera S. 2019. Palaeoclimatic estimates for the late Cenozoic (Mio-Pliocene) Siwalik Flora of Bhutan: Evidence for the development of the South Asian Monsoon in the eastern Himalaya. Palaeogeography, Palaeoclimatology, Palaeoecology 514: 326–335.

Khan M.A., Ghosh R., Bera S., Spicer R.A. & Spicer T.E.V. 2011. Floral diversity during Plio-Pleistocene Siwalik sedimentation (Kimin Formation) in Arunachal Pradesh, India, and its palaeoclimatic significance. Palaeobiodiversity and Palaeoenvironments 91: 237–255.

Khan M.A., Spicer R.A., Bera S., Ghosh R., Yang J., Spicer T.E.V., Guo S., Su T., Jacques F. & Grote P.J. 2014a. Miocene to Pleistocene floras and climate of the eastern Himalayan Siwaliks, and new palaeoelevation estimates for the Namling-Oiyug Basin, Tibet. Global and Planetary Change 113: 1–10.

Khan M.A., Spicer R.A., Spicer T.E.V. & Bera S. 2014b. Fossil evidence of insect folivory in the eastern Himalayan Neogene Siwalik forests. Palaeogeography, Palaeoclimatology, Palaeoecology 410: 264–277.

Kumaravel V., Sangode S.J., Siva Siddaiah T.N. & Rohtash K. 2005. Rock magnetic characterization of pedogenesis under high-energy depositional conditions: a case study from the Mio-Pliocene Siwalik fluvial sequence near Dehradun, NW Himalaya, India. Sedimentary Geology 177: 229–252.

Li S.-F., Valdes P.J., Farnsworth A., Davies-Barnard T., Su T., Lunt D.J., Spicer R.A., Liu J., Deng W.-Y.-D., Huang J., Tang H., Ridgwell A., Chen L.-L. & Zhou Z.-K. 2021. Orographic evolution of northern Tibet shaped vegetation and plant diversity in eastern Asia. Science advances 7: eabc7741.

Li W.Y. & Liang Y.L. 1983. Sporo-pollen analysis on the lacustrine deposits in Zanda Basin during the Pliocene. The Comprehensive Scientific Expedition to the Qinghai–Xizang Plateau, Academia Sinica ed. Quaternary geology in Xizang. Science press, Beijing, pp. 132–144 (in Chinese).

Lourens L.J. 2004. Revised tuning of Ocean Drilling Program Site 964 and KC01B (Mediterranean) and implications for the $\delta^{18}O$, tephra, calcareous nannofossil, and geomagnetic reversal chronologies of the past 1.1 Myr. Paleoceanography19: PA3010.

Medlicott H.B. 1864. On the geological structure and relations of the southern position of Himalayan ranges between the rivers Ganges and Ravee. Memoirs of the Geological Survey of India 3: 1–212.

Meyer H.W. 1992. Lapse rates and other variables applied to estimating paleoaltitudes from fossil floras. Palaeogeography, Palaeoclimatology, Palaeoecology 99: 71–99.

Meyer H.W. 2007. A review of paleotemperature lapse rate methods for estimating paleoelevation from fossil floras. Reviews in Mineralogy and Geochemistry 66: 155–171.

Middlemiss C.S. 1890. Physical geology of the Sub-Himalayas of Garhwal and Kumaon. Memoirs of the Geological Survey of India 24: 59–200.

Mitra S., Bera S. & Banerjee M. 2000. Palynofloral assemblage from Siwalik foredeep Neogene sediments of Darjeeling foothills, Eastern Himalaya. Geophytology 28(1–2): 121–127.

Molnar P. & England P. 1990. Late Cenozoic uplift of mountain ranges and global climate change: chicken or egg? Nature 346(6279): 29–34.

More S., Paruya D.K., Taral S., Chakraborty T. & Bera S. 2016. Depositional environment of Mio-Pliocene Siwalik sedimentary strata from the Darjeeling Himalayan Foothills, India: A palynological approach. PloS One11(3): e0150168.

Mosbrugger V. & Utescher T. 1997. The coexistence approach – a method for quantitative reconstructions of Tertiary terrestrial palaeoclimate data using plant fossils. Palaeogeography, Palaeoclimatology, Palaeoecology 134: 61–86.

Mulch A. 2016. Stable isotope paleoaltimetry and the evolution of landscapes and life. Earth and Planetary Science Letters 433: 180–191.

Mulch A. & Chamberlain C.P. 2006. The rise and growth of Tibet. Nature 439: 670–671.

Mulch A. & Chamberlain C.P. 2018. Stable Isotope Paleoaltimetry: Paleotopography as a Key Element in the Evolution of Landscapes and Life, in: Hoorn C., Perrigo A. & Antonelli A. (Eds.), Mountains, Climate and Biodiversity. Wiley Blackwell, pp. 81–93.

Needham J. 1986. Science and Civilization in China: Volume 3, Mathematics and the Sciences of the Heavens and the Earth. Caves Books Ltd., Taipei.

New M., Lister D., Hulme M. & Makin I. 2002. A high-resolution data set of surface climate over global land areas. Climate Research 21: 1–15.

Pathak N.R. 1969. Megafossils from the foothills of Darjeeling district, India. In: Santapau, H. (Ed.), J. Sen Memorial Volume, Botanical Society Bengal, Calcutta, pp. 379–384.

Peters N.A., Huntington K.W. & Hoke G.D. 2013. Hot or not? Impact of seasonally variable soil carbonate formation on paleotemperature and O-isotope records from clumped isotope thermometry. Earth and Planetary Science Letters 361: 208–218.

Pilgrim G.E. 1913. The correlation of the Siwaliks with mammal horizons of Europe. Records of the Geological Survey of India 43(4): 264–326.

Poage M.A. & Chamberlain C.P. 2001. Empirical relationships between elevation and the stable isotope composition of precipitation and surface waters: considerations for studies of paleoelevation change. American Journal of Science 301: 1–15.

Polissar P., Freeman K., Rowley D.B., McInerney F. & Currie B.S. 2009. Paleoaltimetry of the Tibetan plateau from D/H ratios of lipid biomarkers. Earth and Planetary Science Letters 287: 64–76.

Pound M.J. & Salzmann U. 2017. Heterogeneity in global vegetation and terrestrial climate change during the late Eocene to early Oligocene transition. Scientific Reports 7: 43386. https://doi.org/10.1038/srep43386.

Prasad M. 1994a. Angiospermous leaf remains from the Siwalik sediments of Haridwar, Uttar Pradesh and their bearing on palaeoclimate and phytogeography. Himalayan Geology 15: 83–94.

Prasad M. 1994b. Siwalik (Middle Miocene) woods from the Kalagarh area in the Himalayan foot hills and their bearing on

palaeoclimate and phytogeography. Review of Palaeobotany and Palynology 76: 49–82.

Prasad M. 1994c. Siwalik (Middle Miocene) leaf impressions from the foot-hills of the Himalaya, India. Tertiary Research 15(2): 53–90.

Prasad M. & Pandey S.M. 2008. Plant diversity and climate during Siwalik (Miocene–Pliocene) in the Himalayan foothills of western Nepal. Palaeontographica Abt. B 278: 13–70.

Qian F. 1999. Study on magnetostratigraphy in Qinghai–Tibetan plateau in late Cenozoic. Journal of Geomechanics 5: 22–34.

Qiu J. 2008. The Third Pole. Nature 454: 393–396.

Quade J, Cater J.M.L., Ojha T.P., Adam J. & Harrison T.M. 1995. Late Miocene environmental change and in Nepal and the northern Indian subcontinent; stable isotopic evidence from paleosols: Geological Society of America Bulletin 107: 1381–1397, doi:10.1130/0016-7606.

Quade J., Eiler J., Daëron M. & Achyuthan H. 2013. The clumped isotope geothermometer in soil and paleosol carbonate: Geochimica et Cosmochimica Acta, 105: 92–107, doi:10.1016/j.gca.2012.11.031.

Rowley D.B. & Currie B.S. 2006. Palaeoaltimetry of the late Eocene to Miocene Lunpola Basin, central Tibet. Nature 439: 677–681.

Rowley D.B. & Garzione C.N. 2007. Stable isotope-based paleoaltimetry: Annual Reviews in Earth and Planetary Science 35: 463–508.

Rowley D.B., Pierrehumbert R.T. & Currie B.S. 2001. A new approach to stable isotope-based paleoaltimetry; implications for paleoaltimetry and paleohypsometry of the High Himalaya since the late Miocene. Earth and Planetary Science Letters 188: 253–268.

Sahagian D.L., Proussevitch A. & Carlson W. 2002. Timing of Colorado Plateau uplift: Initial constraints from vesicular basalt-derived paleoelevations. Geology: 30: 807–810.

Sangode S.J., Kumar R. & Ghosh S.K. 2003. Magnetic polarity stratigraphy of the Late Miocene Siwalik group sediments from Kangra Re-entrant, H.P., India. Himalayan Geology 24(1): 47–61.

Sarkar S. 1989. Siwalik pollen succession from Surai Khola of western Nepal and its reflection on paleoecology. Palaeobotanist 38: 319–324.

Saupe E.E., Qiao H., Donnadieu Y., Farnsworth A., Kennedy-Asser A.T., Ladant J.-B., Lunt D.J., Pohl A., Valdes P. & Finnegan S. 2019. Climatic shifts drove major contractions in avian latitudinal distributions throughout the Cenozoic. Proceedings of the National Academy of Sciences 116: 12895–12900.

Saylor J.E., Quade J., Dellman D.L., DeCelles P.G., Kapp P.A. & Ding L. 2009. The late Miocene through present paleoelevation history of southwestern Tibet. American Journal of Science 309: 1–42.

Spicer R.A. 1981. The Sorting and Deposition of Allochthonous Plant Material in a Modern Environment at Silwood Lake, Silwood Park, Berkshire, England. US Geological Survey Professional Paper 1143: 1–77.

Spicer R.A. 2018. Phytopaleoaltimetry: Using Plant Fossils to Measure Past Land Surface Elevation, in Mountains, Climate and Biodiversity, Hoorn C., Perrigo A & Antonelli A Eds. (Wiley-Blackwell 2018), chap. 7, pp. 96–109.

Spicer R.A., Harris N.B.W., Widdowson M., Herman A.B., Guo S., Valdes P.J., Wolfe J.A. & Kelley S.P. 2003. Constant elevation of Southern Tibet over the past 15 million years. Nature 412: 622–624.

Spicer R.A., Su T., Valdes P.J., Farnsworth A., Wu F.-X., Shi G., Spicer T.E.V. & Zhou Z.-K. 2020a. The Topographic Evolution of the Tibetan Region as Revealed by Palaeontology. Palaeobiodiversity and Palaeoenvironments101: 213–243, https://doi.org/10.1007/s12549-020-00452-1

Spicer R.A., Yang J., Spicer T.E.V. & Farnsworth A. 2020b.Woody dicot leaf traits as a palaeoclimate proxy: 100 years of development and application. Palaeogeography, Palaeoclimatology, Palaeoecology 562: 110138, https://doi.org/10.1016/j.palaeo.2020.110138

Srivastava G., Paudayal K.N., Utescher T. & Mehrotra R.C. 2018. Miocene vegetation shift and climate change: Evidence from the Siwalik of Nepal. Global and Planetary Change 161: 108–120.

Su T., Farnsworth A., Spicer R.A., Huang J., Wu F.-X., Liu J., Li S.-F., Xing Y.-W., Huang Y.-J., Deng W.-Y.-D., Tang H., Xu C.-L., Zhao F., Srivastava G., Valdes P.J., Deng T. & Zhou Z.-K. 2019. No high Tibetan Plateau until the Neogene. Science Advances 5: eaav2189.

Su T., Spicer R.A., Wu F.-X., Farnsworth A., Huang J., Del Rio C., Deng T., Ding L., Deng W.-Y.-D., Huang Y.-J., Hughes A., Jia L.-B., Jin J.-H., Li S.-F., Liang S.-Q., Liu J., Liu X.-Y., Sherlock S., Spicer T., Srivastava G., Tang H., Valdes P., Wang T.-X., Widdowson M., Wu M.-X., Xing Y.-W., Xu C.-L., Yang J., Zhang C., Zhang S.-T., Zhang X.-W., Zhao F. & Zhou Z.-K. 2020. A Middle Eocene lowland humid subtropical "Shangri-La" ecosystem in central Tibet. PNAS 117: 32989–32995.

Taft L., Wiechert U., Zhang H.C., Lei G.L., Mischke S., Plessen B., Weynell M., Winkler A. & Riedel F. 2013. Oxygen and carbon isotope patterns archived in shells of the aquatic gastropod *Radix*: Hydrologic and climatic signals across the Tibetan Plateau in sub-monthly resolution. Quaternary International 290: 282–298, doi:10.1016/j.quaint .2012.10.031.

Tapponnier P., Xu Z.Q., Roger F., Meyer B., Arnaud N., Wittlinger G. & Yang J. 2001. Oblique stepwise rise and growth of the Tibet Plateau. Science 294: 1671–1677.

The Comprehensive Scientific Expedition to the Qinghai–Xizang Plateau, Academia Sinica ed. Forests of Xizang. Beijing: Science Press, 1985: 38–266 (in Chinese).

Thomas J.V., Parkash B. & Mohindra R. 2002. Lithofacies and palaeosol analysis of the Middle and Upper Siwalik Groups (Plio-Pleistocene), Haripur-Kolar section, Himachal Pradesh, India: Sedimentary Geology 150: 343–366, doi:10.1016/S0037-0738 (01) 00203-2.

Thompson L.G., Yao T., Mosley-Thompson E., Davis M.E., Henderson K.A. & Lin P.N. 2000. A high-resolution millennial record of the South Asian Monsoon from Himalayan ice cores: Science 289: 1916–1919, doi:10.1126/science.289.5486.1916.

Utescher T., Bruch A.A., Erdei B., François L., Ivanov D., Jacques F.M.B., Kern A.K., Liu Y.-S.(C), Mosbrugger V. & Spicer R.A. 2014. The Coexistence Approach—Theoretical background and practical considerations of using plant fossils for climate quantification. Palaeogeography, Palaeoclimatology, Palaeoecology 410: 58–73.

Valdes P.J., Armstrong E., Badger M.P.S., Bradshaw C.D., Bragg F., Crucifix M., Davies-Barnard T., Day J.J., Farnsworth A., Gordon C., Hopcroft P.O., Kennedy A.T., Lord N.S., Lunt D.J., Marzocchi A., Parry L.M., Pope V., Roberts W.H.G., Stone E.J., Tourte

G.J.L. & Williams J.H.T. 2017. The BRIDGE HadCM3 family of climate models: HadCM3@Bristol v1.0. Geoscientific Model Development 10: 3715–3743.

Wang C., Zhao X., Liu Z., Lippert P.C. , Graham S.A., Coe R.S., Yi H., Zhu L., Liu S. & Li Y. 2008. Constraints on the early uplift history of the Tibetan Plateau. Proceedings of the National Academy of Sciences, USA 105: 4987–4992, doi:doi/10.1073/pnas.0703595105.

Wang C.S., Dai J., Zhao X., Li Y., Graham S.A., He D., Ran B. & Meng J. 2014. Outward growth of the Tibetan plateau during the Cenozoic: a review. Tectonophysics 621: 1–43.

Wang S., Zhang W., Fang X., Dai S. & Kempf O. 2008. Magnetostratigraphy of the Zanda Basin in southwest Tibet Plateau and its tectonic implications. China Science Bulletin 53: 1393–1400.

Wang X.M., Li Q., Xie G.P., Saylor J.E., Tseng Z.J., Takeuchi G.T., Deng T., Wang Y., Hou S.K., Liu J., Zhang C.F., Wang N. & Wu F.X. 2013. Mio-Pleistocene Zanda Basin biostratigraphy and geochronnology, pre-Ice Age fauna, and mammalian evolution in western Himalaya. Palaeogeography, Palaeoclimatology, Palaeoecology 374: 81–95.

Wolfe J.A. 1992. An analysis of Present-day terrestrial lapse rates in western conterminous United states and their significance to paleoaltitudinal estimates. US Geological Survey Bulletin 1964: 1–35, pl 1–2.

Wu F., Herrmann M. & Fang X. 2014. Early Pliocene paleoaltimetry of the Zanda Basin indicated by a sporopollen record. Palaeogeography, Palaeoclimatology, Palaeoecology 412: 261–268.

Xiong Z., Liu X., Ding L., Farnsworth A., Spicer R.A., Xu Q., Valdes P., He S., Zeng D., Wang C., Li Z., Guo X., Su T., Zhao C., Wang H. & Yue Y. 2022. The rise and demise of the Paleogene Central Tibetan Valley. Science Advances 8(6): eabj0944.

Zaarur S., Olack G. & Affek H.P. 2011. Paleoenvironmental implication of clumped isotopes in land snail shells. Geochimica et Cosmochimica Acta75: 6859–6869,doi: 10.1016/j.gca.2011.08.044.

Zachos J., Pagani M., Sloan L., Thomas E. & Billups K. 2001. Trends, rhythms, and aberrations in global climate 65 Ma to present. Science 292: 686–693, doi:10.1126/science.1059412.

Zhang Q., Wang F., Ji H. & Huang W. 1981. Pliocene sediments of the Zanda Basin, Tibetan Journal of Stratigraphy 5: 216–220.

Zhang Y., Kong Z., Yang Z., Wang L. & Duan X. 2017. Surface pollen distribution from Alpine vegetation in Eastern Tibet, China. Scientific Reports 7: 586 https://doi.org/10.1038/s41598-017-00625-7.